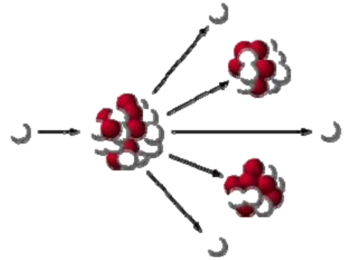

The use of MonteCarlo radiation transport codes in radiation physics and dosimetry: part II, modeling of nuclear reactions

Alfredo Ferrari
CERN, Geneva Switzerland

CERN, 28 June 2006

Disclaimer:

A significant fraction of the examples presented in this lecture is based on the work of many colleagues: in particular

F.Ballarini, G.Battistoni, M.Brugger, F.Cerutti, R.Engel, A.Fassò, M.V.Garzelli, K.Parodi, M.Pelliccioni, J.Ranft, S.Roesler, P.R.Sala, F.Sommerer, V.Vlachoudis,

and many others, mostly but not only from the FLUKA collaboration

Most of the examples presented have been obtained with the FLUKA code, the speaker is one of the authors of, which is the tool used at CERN for most radioprotection/dosimetry calculations

They are representative of state-of-the-art nuclear models and should give a reasonable insight into the underlying physics concepts

Outline

- Introduction
  - Hadronic physics vs MonteCarlo
  - Nuclear interaction vs dosimetry and radiation protection
- Nuclear interactions in brief
  - Hadron-Nucleon & Hadron-Nucleus
  - Nucleus-Nucleus
  - Real and Virtual Photonuclear interactions
- Examples of applications
  - Activity and residual dose rate predictions
  - Cosmic rays, commercial flights and missions to MARS
  - Hadrotherapy applications

HEP Hadronic MC applications:

MC simulations are a well established tool in HEP for:

- Particle physics: calorimetry, tracking and detector simulation
- Accelerator design ($\rightarrow$ LHC systems)
- Radiation protection (shielding, activation, …)
- Dosimetry
- Cosmic ray physics

They are also used for:

- ➢ Neutronics simulations
- ➢ ADS (Accelerator Driven Systems)

Applications to Medicine/radiobiology are growing, thanks to

- ✓ Mixed field capability, including ion transport and interactions
- ✓ Accuracy
- ✓ Reliability

Inelastic hN interactions

Intermediate Energies

- $N_1 + N_2 \rightarrow N_1' + N_2' + \pi$ threshold around 290 MeV
  important above 700 MeV
- $\pi + N \rightarrow \pi' + \pi'' + N'$ opens at 170 MeV

- Dominance of the $\Delta(1232)$ resonance and of the N* resonances $\rightarrow$ reactions treated in the framework of the isobar model $\rightarrow$ all reactions proceed through an intermediate state containing at least one resonance
- Resonance energies, widths, cross sections, branching ratios from data and conservation laws, whenever possible

High Energies: Dual Parton Model/Quark Gluon String Model etc

- Interacting strings (quarks held together by the gluon-gluon interaction into the form of a string)
- Interactions treated in the Reggeon-Pomeron framework
- each of the two hadrons splits into 2 colored partons $\rightarrow$ combination into 2 colourless chains $\rightarrow$ 2 back-to-back jets
- each jet is then hadronized into physical hadrons

Hadron-Nucleon Cross Section

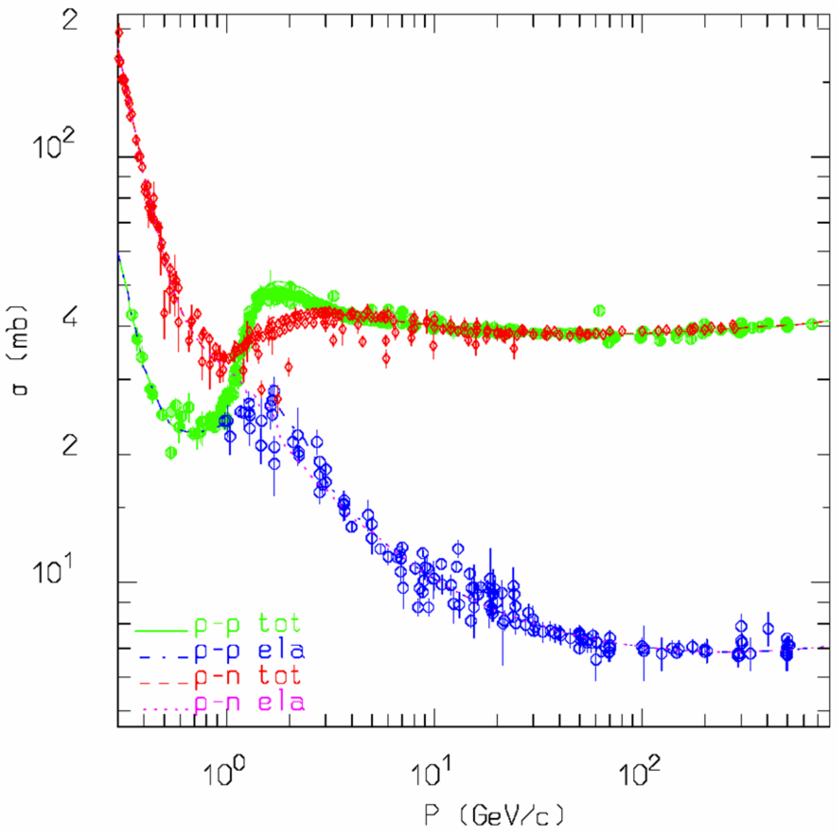

Total and elastic cross section for p-p and p-n scattering, together with experimental data

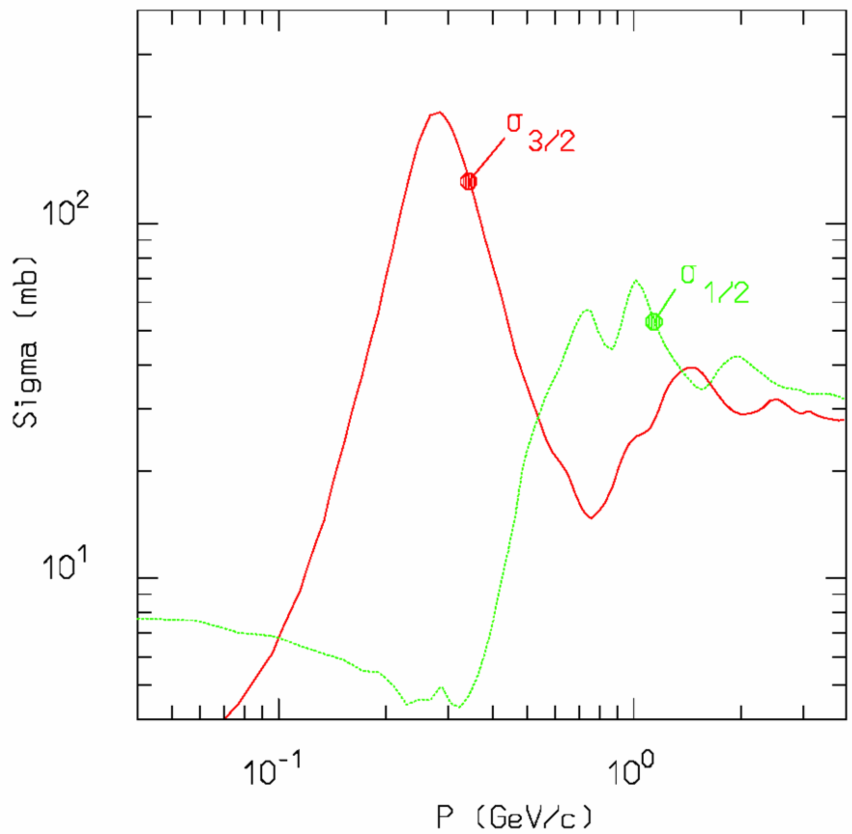

Isospin decomposition of π-nucleon cross section in the T=3/2 and T=1/2 components

Hadronic interactions are mostly surface effects $\Rightarrow$ hadron nucleus cross section scale with the target atomic mass $A^{2/3}$

Inelastic hN at high energies (DPM)

Parton and color concepts, Topological expansion of QCD, Duality

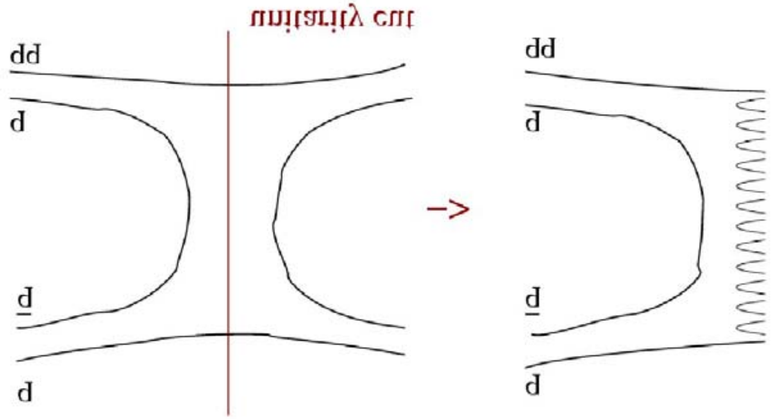

Reggeon exchange

color strings to be "hadronized"

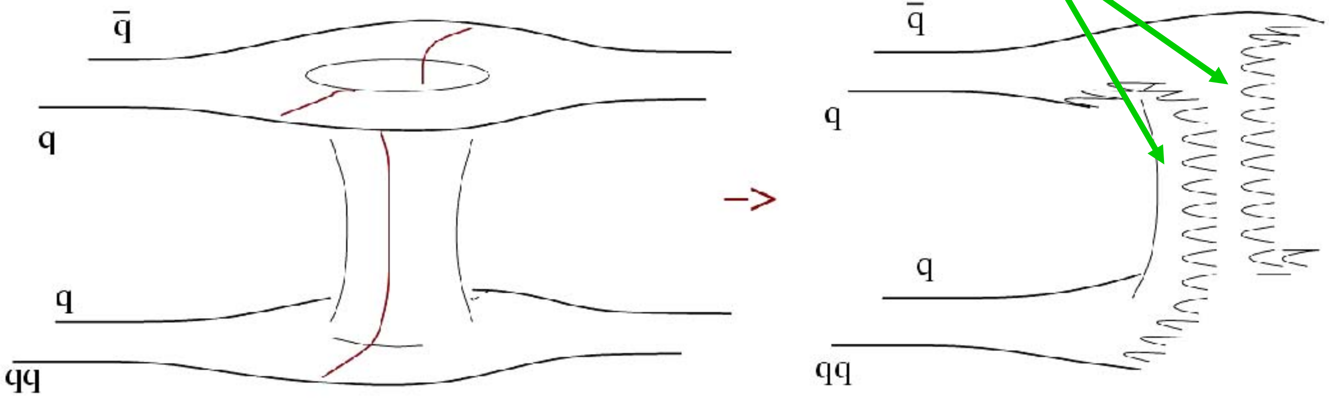

Pomeron exchange

Hadron-hadron collisions: chain examples

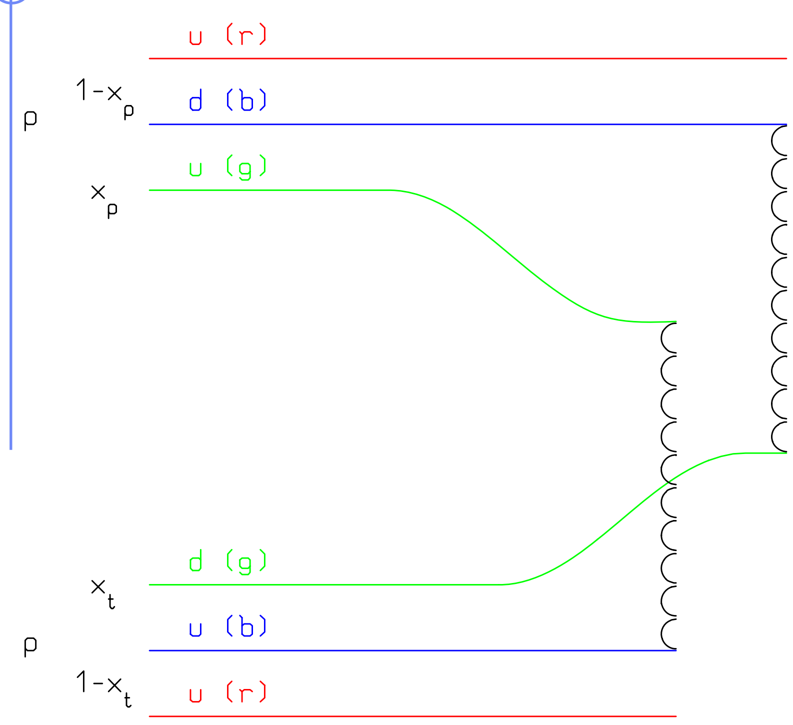

Leading two-chain diagram in DPM for p-p scattering. The color (red, blue, and green) and quark combination shown in the figure is just one of the allowed possibilities

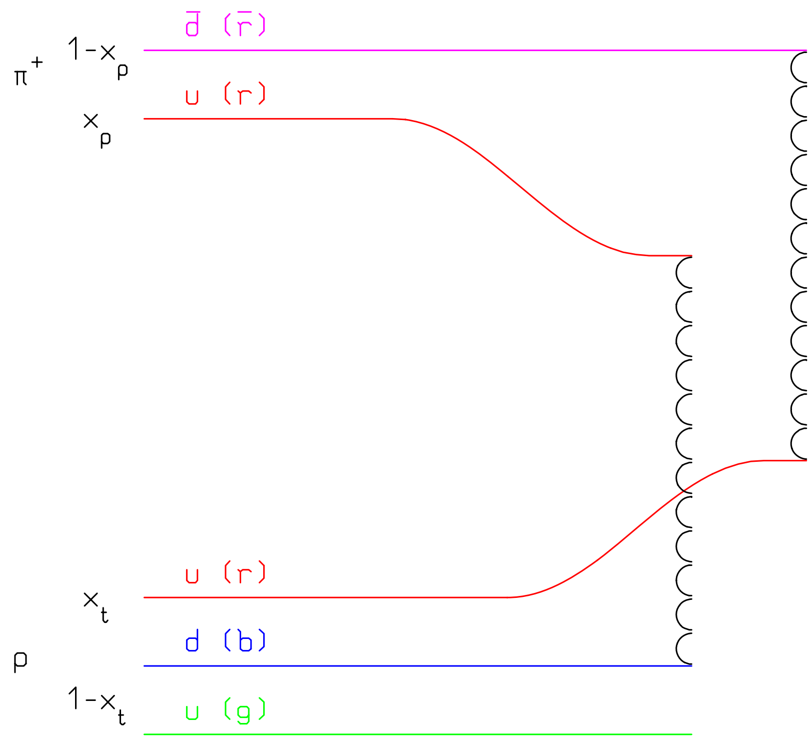

Leading two-chain diagram in DPM for π^+-p scattering. The color (red, blue, and green) and quark combination shown in the figure is just one of the allowed possibilities

The "hadronization" of color strings

An example:

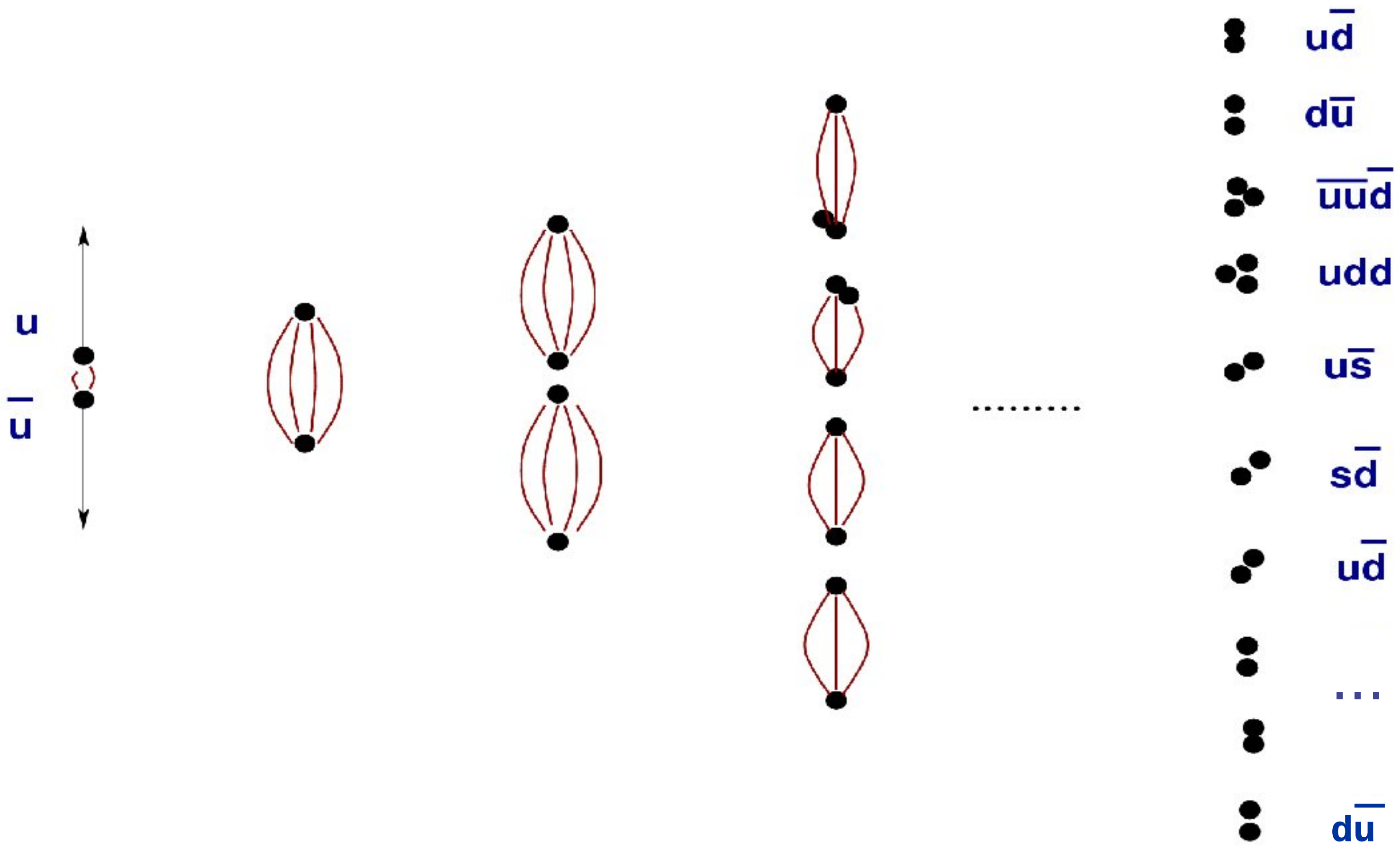

Inelastic hN interactions: examples

$\pi^+ + p \rightarrow \pi^+ + X$ (6 & 22 GeV/c)

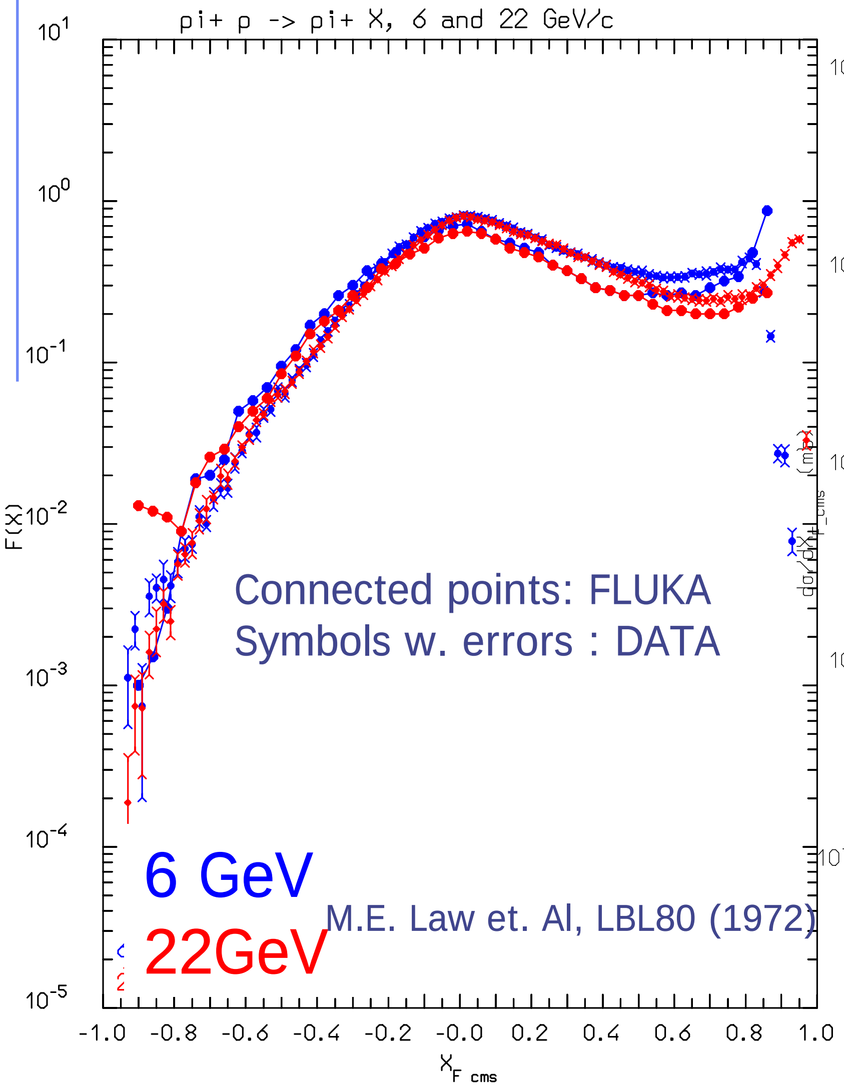

$\pi^+ + p \rightarrow Ch^+/Ch^- + X$ (250 GeV/c)

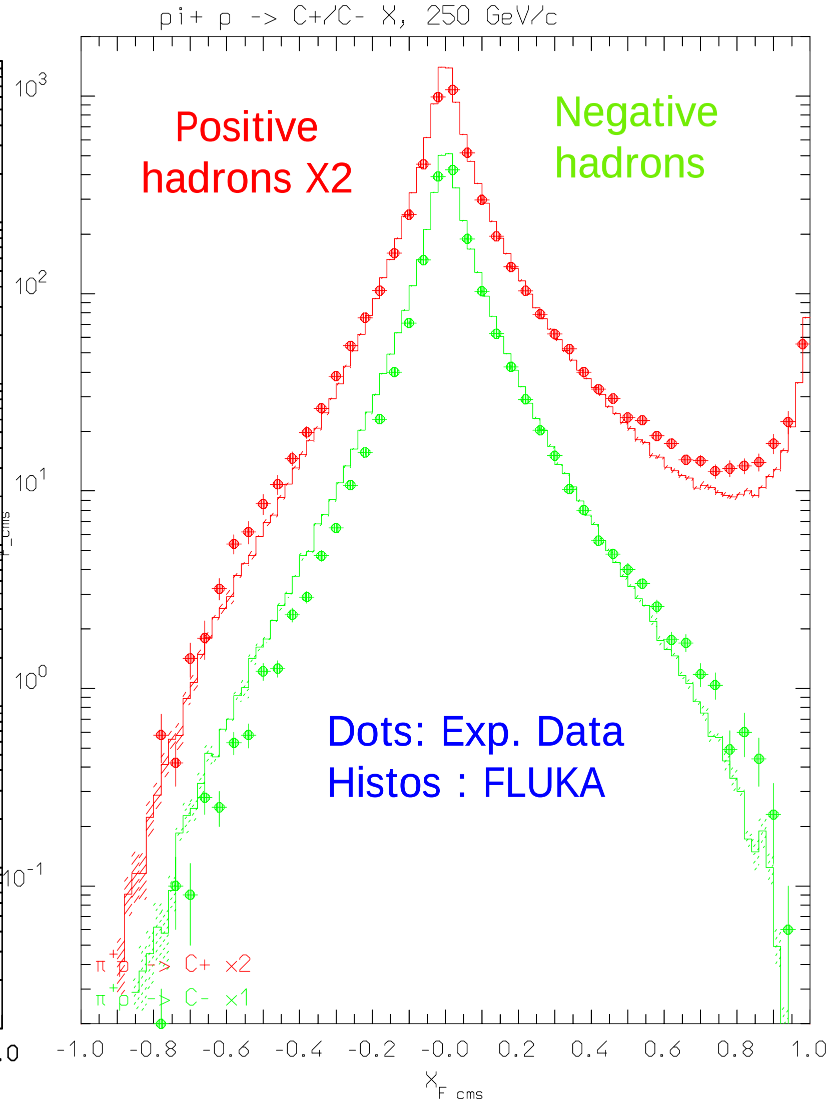

MC modeling of nuclear interactions:

Target nucleus description (density, Fermi motion, etc)

⇩

Glauber-Gribov cascade with formation zone

⇩

(Generalized) IntraNuclear cascade

⇩

Preequilibrium stage with current exciton configuration and excitation energy
(all non-nucleons emitted/decayed + all nucleons below 30-100 MeV)

⇩

Evaporation/Fragmentation/Fission model

⇩

γ deexcitation

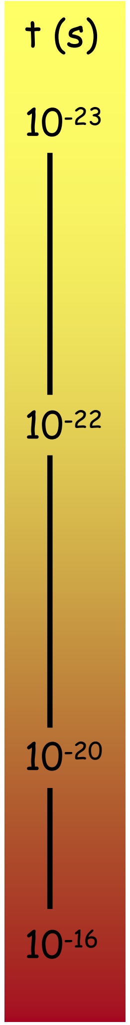

Nucleon Fermi Motion

- Fermi gas model: Nucleons = Non-interacting Constrained Fermions

  Momentum distribution $\propto \frac{dN}{dk} = \frac{|k|^2}{2\pi^2}$

  for *k* up to a (local) Fermi momentum $k_F(r)$ given by

$$k_F(r) = \left[3\pi^2 \rho_N(r)\right]^{\frac{1}{3}}$$

The Fermi energy ($k_F \approx 1.36$ fm, $P_F \approx 260$ MeV/c, $E_F \approx 35$ MeV, at nuclear max. density) is customarily used in building a self-consistent Nuclear Potential

$\Downarrow$

Depth of the potential well ≡ Fermi Energy + Nuclear Binding Energy

(Generalized) IntraNuclear Cascade

- Primary and secondary particles moving in the nuclear medium
- Target nucleons motion and nuclear well according to the Fermi gas model
- Interaction probability

  σ_{free} + Fermi motion × $\rho(r)$ + exceptions (ex. π)
- Glauber cascade at higher energies
- Classical trajectories (+) nuclear mean potential (resonant for π)
- Curvature from nuclear potential $\rightarrow$ refraction and reflection
- Interactions are incoherent and uncorrelated
- Interactions in projectile-target nucleon CMS $\rightarrow$ Lorentz boosts
- Multibody absorption for π, μ^-, K^-
- Quantum effects (Pauli, formation zone, correlations…)
- Exact conservation of energy, momenta and all addititive quantum numbers, including nuclear recoil

Advantages and Limitations of (G)INC

Advantages

- No other model available for energies above the pion threshold production (except QMD models)
- No other model for projectiles other than nucleons
- Easily available for on-line integration into transport codes
- Every target-projectile combination without any extra information
- Particle-to-particle correlations preserved
- Valid on light and on heavy nuclei
- Capability of computing cross sections, even when they are unknown

Limitations

- Low projectile energies E<200MeV are badly described *(partially solved in GINC+preequilibrium)*
- Quasi electric peaks above 100MeV are usually too sharp
- Coherent effect as well as direct transitions to discrete states are not included
- Nuclear medium effects, which can alter interaction properties are not taken into account *(partially solved in GINC)*
- Multibody processes (i.e. interaction on nucleon clusters) are not included *(solved in GINC)*
- Composite particle emissions (d,t,^{3}He,α) cannot be easily accommodated into INC, but for the evaporation stage *(solved in GINC through coalescence)*
- Backward angle emission poorly described *(solved in GINC)*

hA at high energies: Glauber-Gribov cascade with formation zone

- Glauber cascade
  - Quantum mechanical method to compute Elastic, Quasi-elastic and Absorption hA cross sections from Free hadron-nucleon scattering + nuclear ground state
  - Multiple Collision expansion of the scattering amplitude
- Glauber-Gribov
  - Field theory formulation of Glauber model
  - Multiple collisions $\leftrightarrow$ Feynman diagrams
  - High energies: exchange of one or more Pomerons with one or more target nucleons (a closed string exchange)
- Formation zone (=materialization time)

Glauber Cascade

Quantum mechanical method to compute all relevant hadron-nucleus cross sections from hadron-nucleon scattering: $S_{hN}(\vec{b},s) = e^{i\chi_{hN}(\vec{b},s)} = \eta_{hN}(\vec{b},s)e^{2i\delta_{hN}(\vec{b},s)}$

and nuclear ground state wave function Ψ_i

Total $$\sigma_{hA\,T}(s) = 2\int d^2\vec{b}\int d^3\vec{u}\left|\Psi_i(\vec{u})\right|^2\left[1-\prod_{j=1}^{A}\mathrm{Re}\,S_{hN}(\vec{b}-\vec{r}_{j\perp},s)\right]$$

Elastic $$\sigma_{hA\,el}(s) = \int d^2\vec{b}\left|\int d^3\vec{u}\left|\Psi_i(\vec{u})\right|^2\left[1-\prod_{j=1}^{A}S_{hN}(\vec{b}-\vec{r}_{j\perp},s)\right]\right|^2$$

Scattering $$\sigma_{hA\,\Sigma f}(s) \equiv \sum_f \sigma_{hA\,fi}(s) = \int d^2\vec{b}\int d^3\vec{u}\left|\Psi_i(\vec{u})\right|^2\left|\left[1-\prod_{j=1}^{A}S_{hN}(\vec{b}-\vec{r}_{j\perp},s)\right]\right|^2$$

Absorption (particle prod.)

Absorption probability over a given *b* and nucleon configuration

$$\sigma_{hA\,abs}(s) \equiv \sigma_{hA\,T}(s) - \sigma_{hA\,\Sigma f}(s)$$

$$= \int d^2\vec{b}\int d^3\vec{u}\left|\Psi_i(\vec{u})\right|^2\left\{1-\left\{\prod_{j=1}^{A}1-\left[1-\left|S_{hN}(\vec{b}-\vec{r}_{j\perp},s)\right|^2\right]\right\}\right\}$$

Glauber cross section calculations

Self-consistent calculation including "a priori" inelastic screening through the substitution where λ is the ratio of the single diffractive amplitude, 1 side only, over the elastic amplitude

$$\Gamma(s,\vec{b}) \rightarrow \hat{\Gamma}_{hN}(s,\vec{b}) = \begin{bmatrix} 1 & \lambda \\ \lambda & 1 \end{bmatrix} \Gamma_{hN}(s,\vec{b})$$

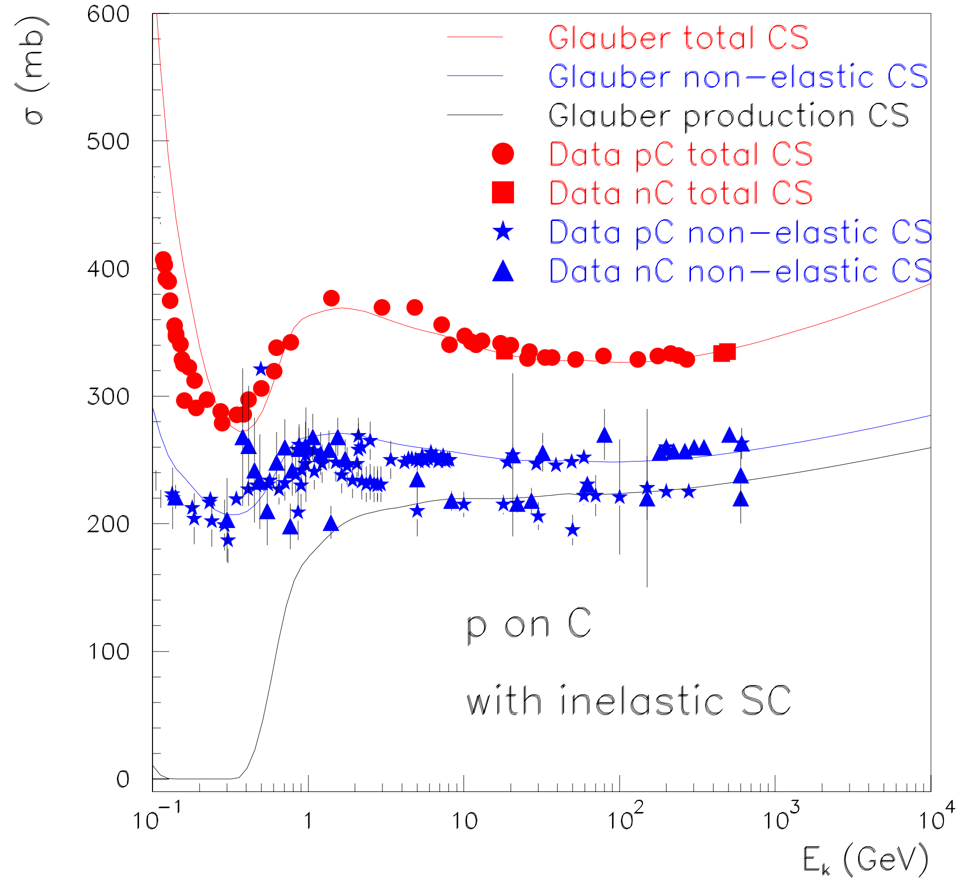

Proton Carbon cross sections with inelastic screening accounted for

Please note the ambiguity of the non-elastic exp. results, almost 2-population like

Gribov interpretation of Glauber multiple collisions

Therefore the absorption cross section is just the integral in the impact parameter plane of the probability of getting at least one non-elastic hadron-nucleon collision

and the overall average number of collision is given by

$$\langle \nu \rangle = \frac{Z\sigma_{hpr} + N\sigma_{hnr}}{\sigma_{hAabs}}$$

- Glauber-Gribov model = Field theory formulation of Glauber model
- Multiple collision terms $\Rightarrow$Feynman graphs
- At high energies : exchange of one or more pomerons with one or more target nucleons

- In the Dual Parton Model language: (neglecting higher order diagrams):

Interaction with ***n*** target nucleons $\Rightarrow$ ***2n*** chains

- Two chains from projectile valence quarks + valence quarks of one target nucleon $\Rightarrow$valence-valence chains
- 2(n-1) chains from sea quarks of the projectile + valence quarks of target nucleons $\Rightarrow$2(n-1) sea-valence chains

Glauber-Gribov: chain examples

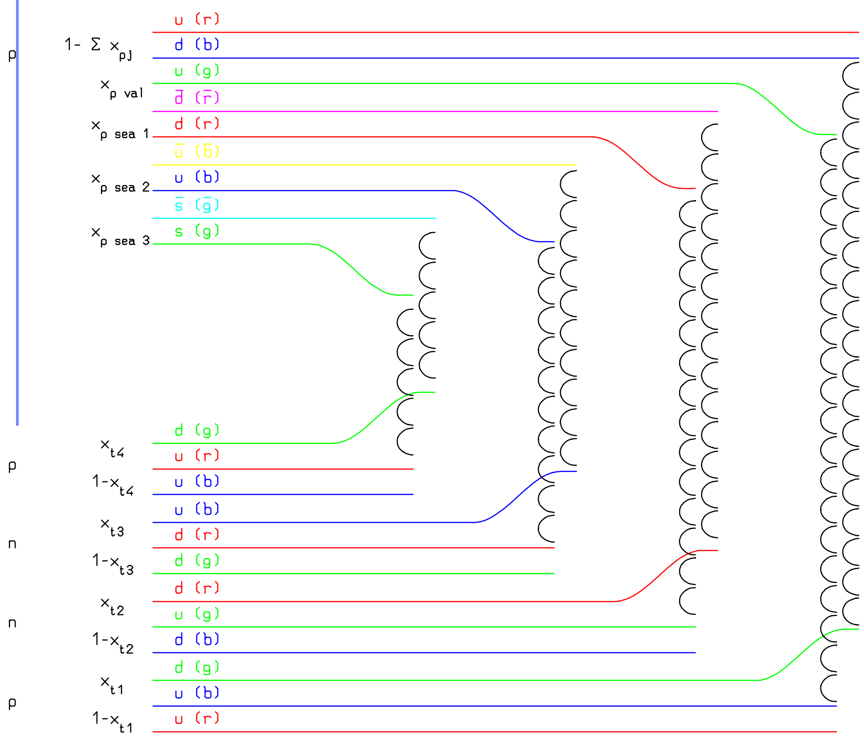

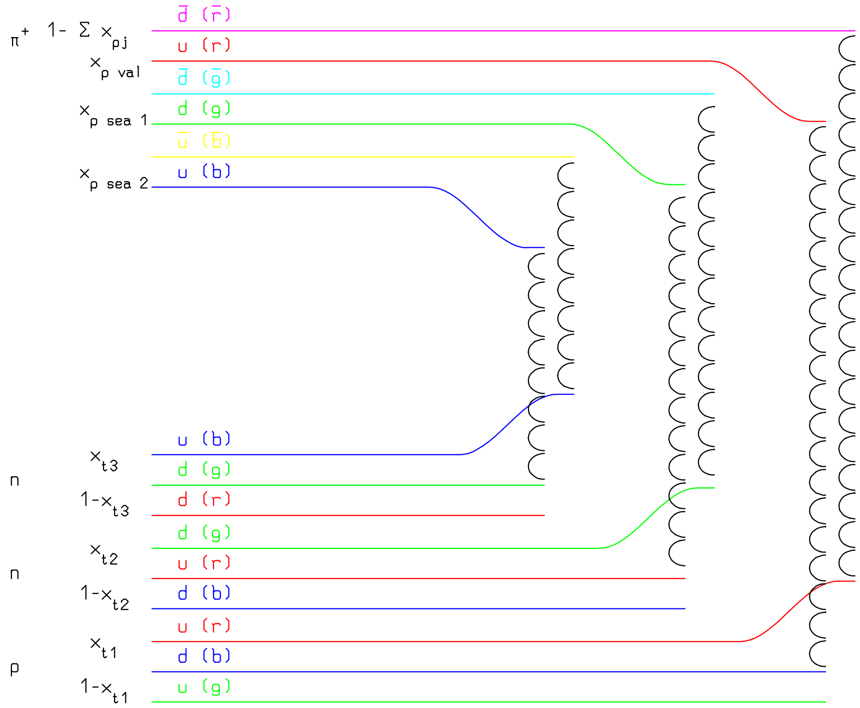

Leading two-chain diagrams in DPM for *p-A* Glauber scattering with 4 collisions. The color (red blue green) and quark combinations shown in the figure are just one of the allowed possibilities

Leading two-chain diagrams in DPM for π^{+-}*A* Glauber scattering with 3 collisions.

From one to many

While the Glauber analytical calculation of cross sections is accurate down to sub-GeV energy, the interpretation in terms of explicit multiple collisions and its MonteCarlo implementation are less sound for projectile energies < 5-10 GeV

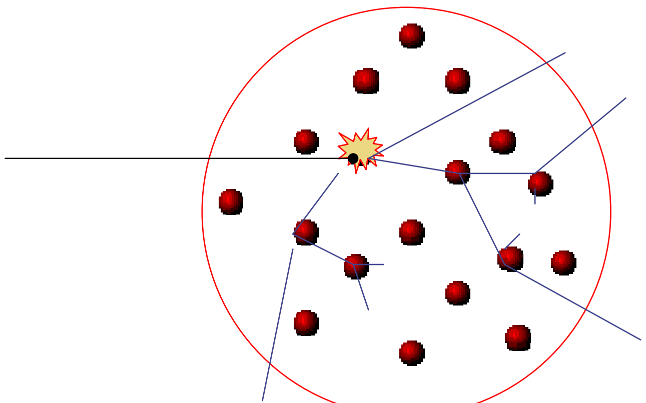

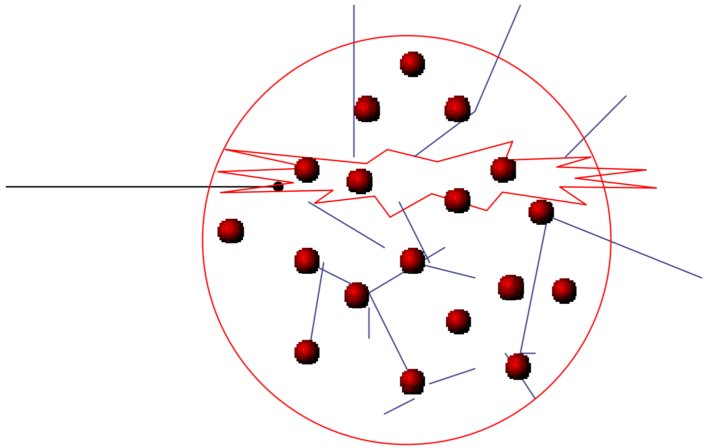

Formation zone

Naively: "materialization" time (originally proposed by Stodolski).
Qualitative estimate:

In the frame where *p// =0*

$$\bar{t} = \Delta t \approx \frac{\hbar}{E_T} = \frac{\hbar}{\sqrt{p_T^2 + M^2}}$$

Particle proper time

$$\tau = \frac{M}{E_T}\bar{t} = \frac{\hbar M}{p_T^2 + M^2}$$

Going to the nucleus system

$$\Delta x_{for} \equiv \beta\, c \cdot t_{lab} \approx \frac{p_{lab}}{E_T}\bar{t} \approx \frac{p_{lab}}{M}\tau = k_{for}\frac{\hbar p_{lab}}{p_T^2 + M^2}$$

Condition for possible reinteraction inside a nucleus:

$$\Delta x_{for} \leq R_A \approx r_0 A^{\frac{1}{3}}$$

Setting the formation zone: no Glauber, no formation zone

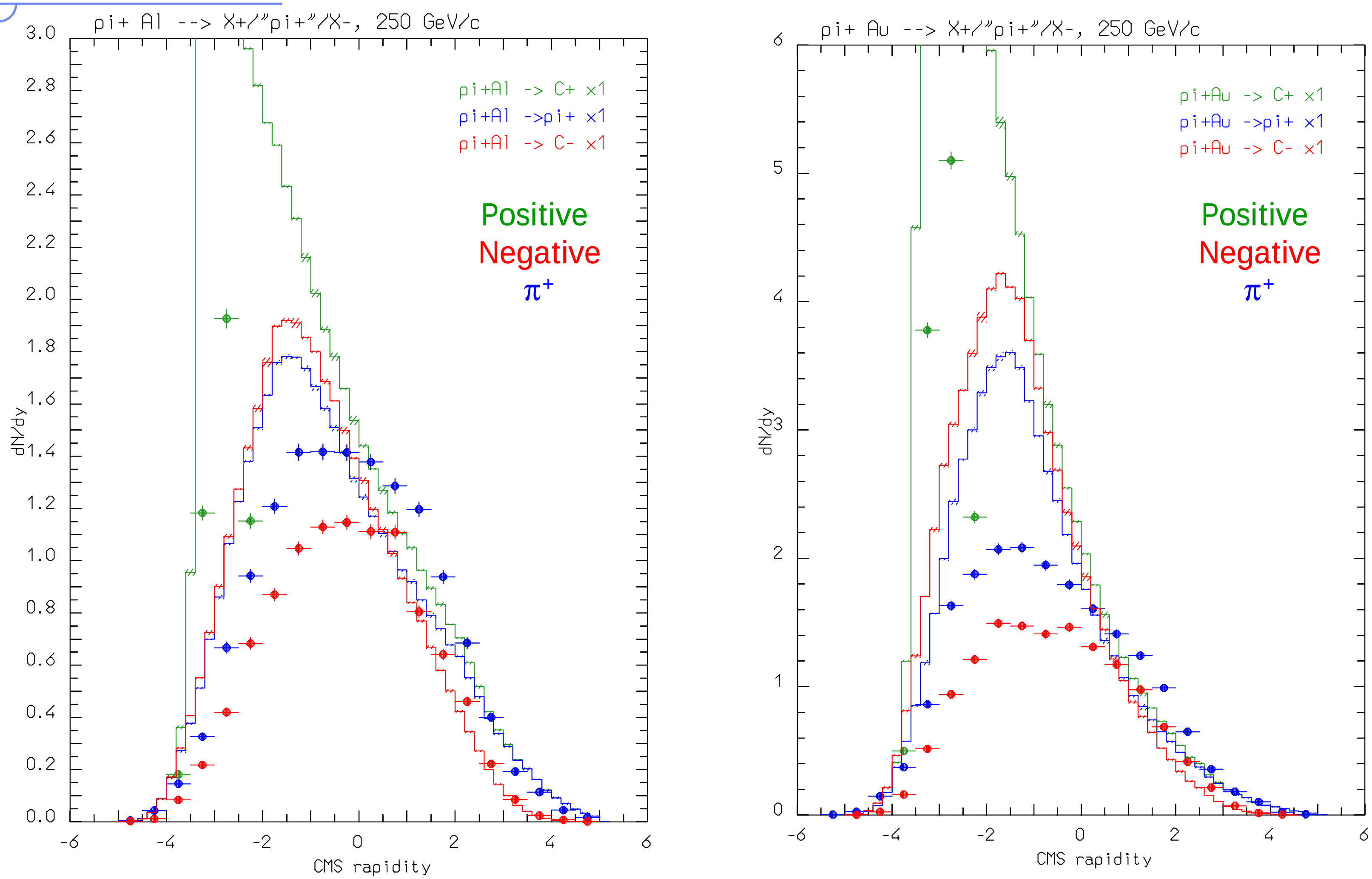

Rapidity distribution of charged particles produced in 250 GeV π^+ collisions on Aluminum (left) and Gold (right)
Points: exp. data (Agababyan et al., ZPC50, 361 (1991)).

Setting the formation zone: no Glauber, yes formation zone

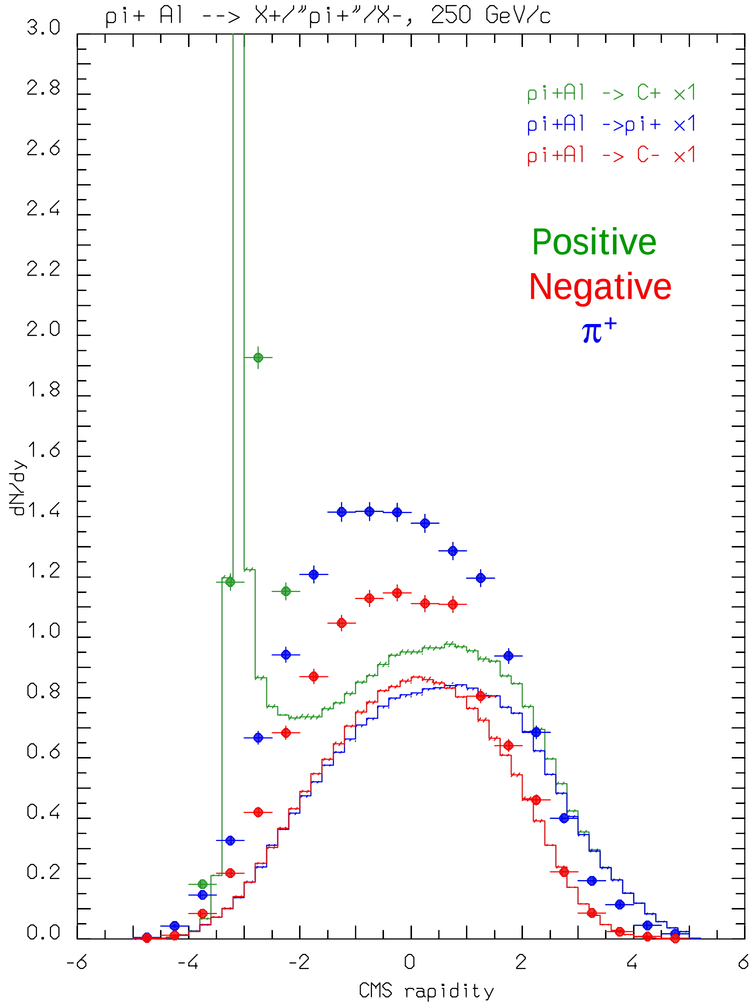

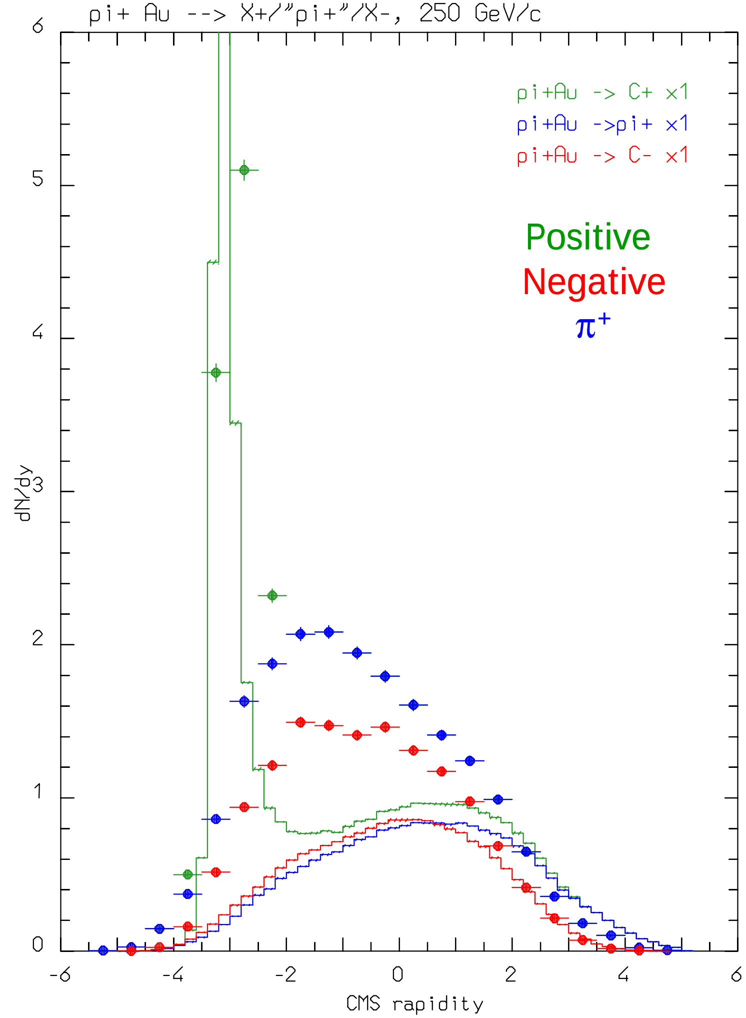

Rapidity distribution of charged particles produced in 250 GeV π^+ collisions on Aluminum (left) and Gold (right)
Points: exp. data (Agababyan et al., ZPC50, 361 (1991)).

Setting the formation zone: yes Glauber, no formation zone

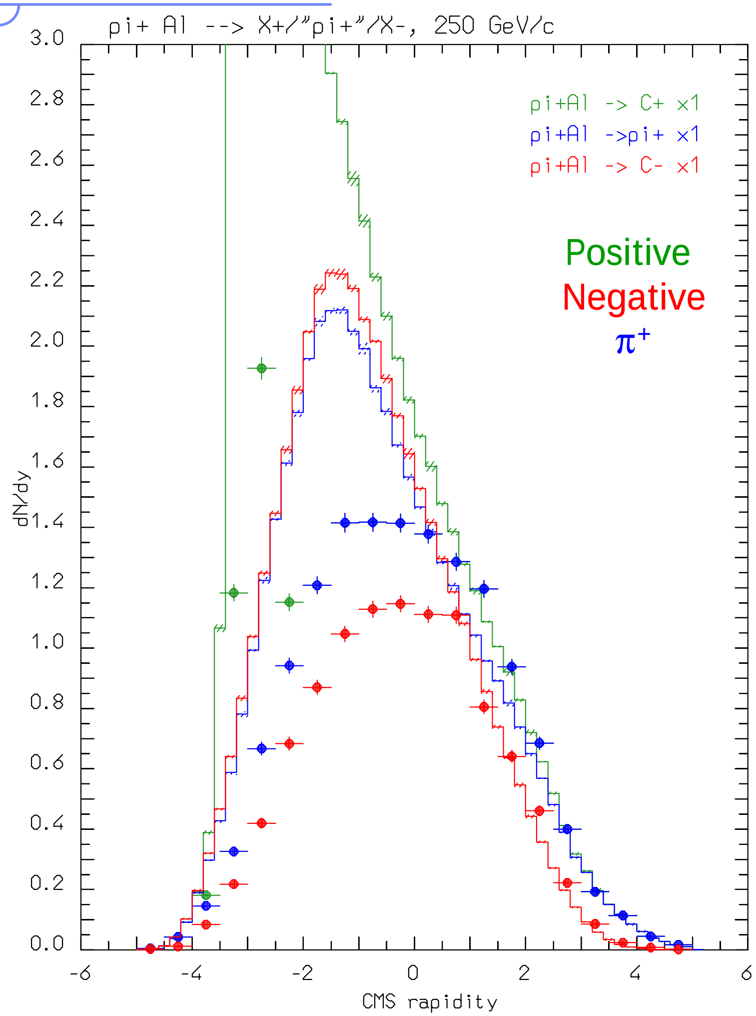

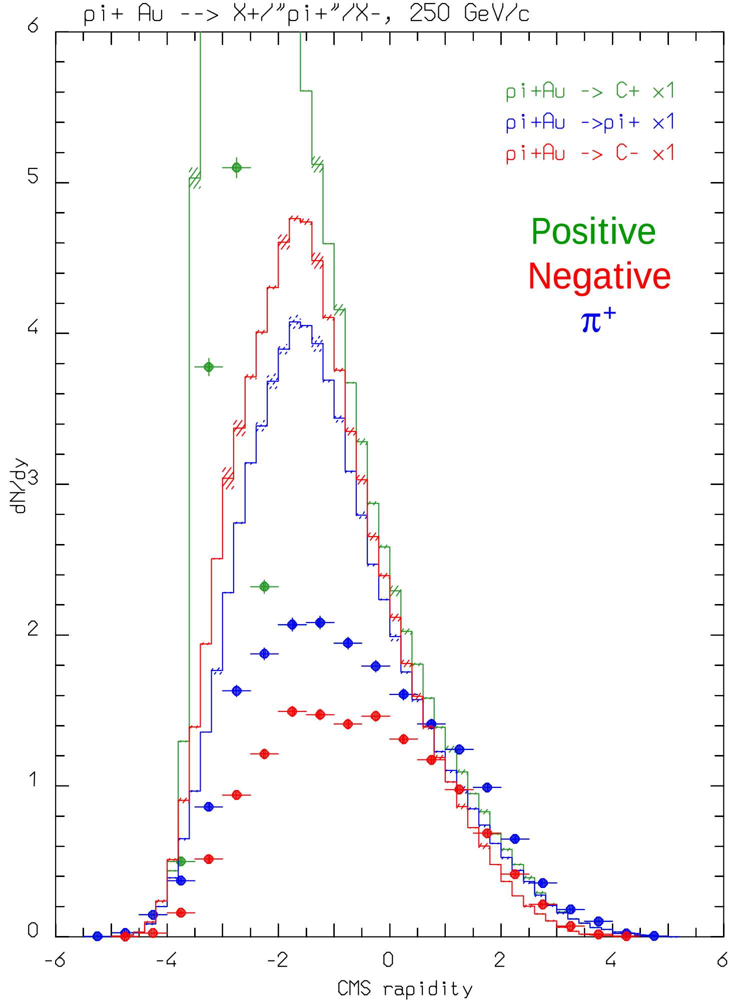

Rapidity distribution of charged particles produced in 250 GeV π^+ collisions on Aluminum (left) and Gold (right)
Points: exp. data (Agababyan et al., ZPC50, 361 (1991)).

Setting the formation zone: yes Glauber, yes formation zone

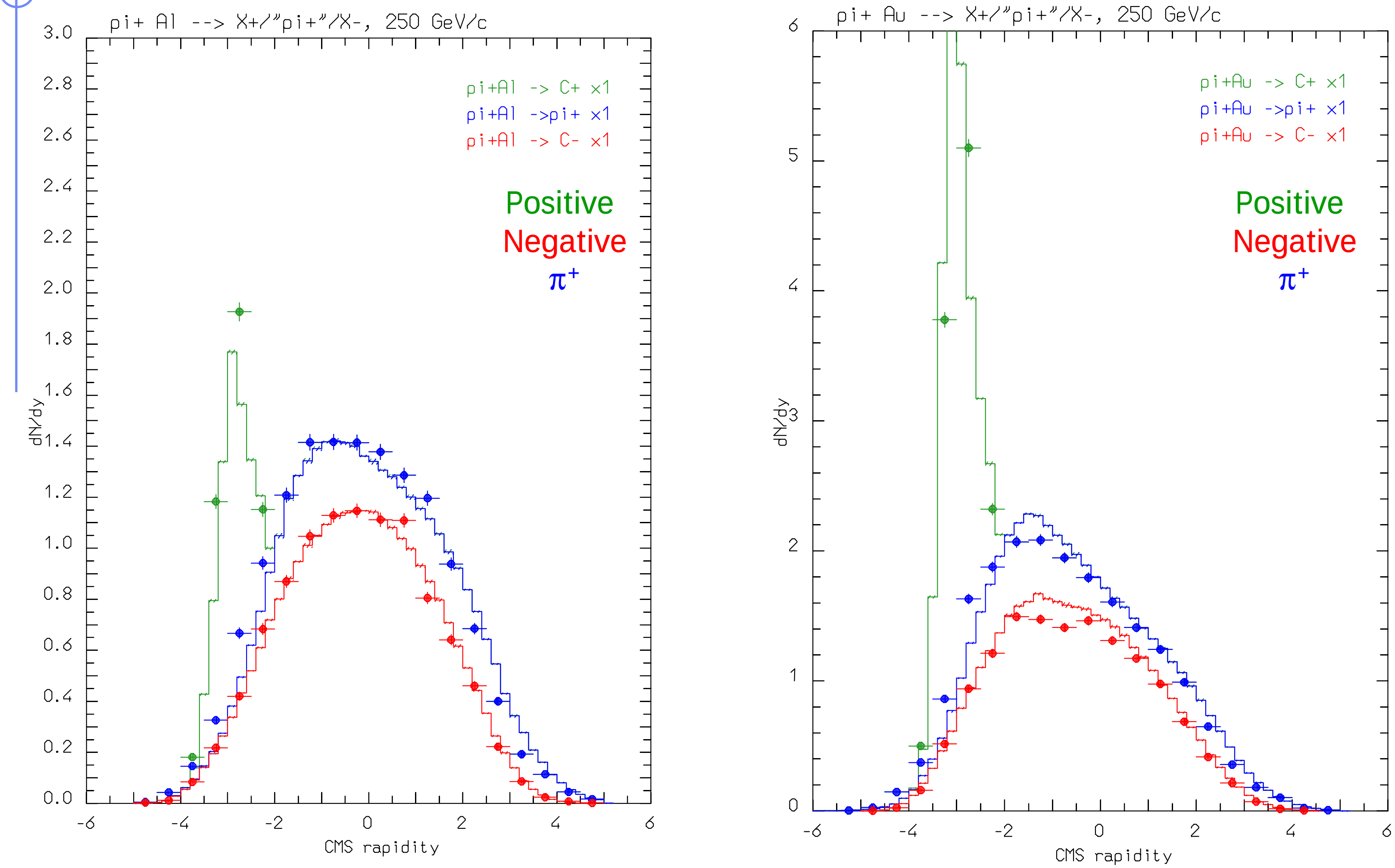

Rapidity distribution of charged particles produced in 250 GeV π^+ collisions on Aluminum (left) and Gold (right)
Points: exp. data (Agababyan et al., ZPC50, 361 (1991)).

Preequilibrium emission

For E > π production threshold $\rightarrow$ only (G)INC models
At lower energies a variety of preequilibrium models

Two leading approaches

The quantum-mechanical multistep model:
Very good theoretical background
Complex, difficulties for multiple emissions

The semiclassical exciton model
Statistical assumptions
Simple and fast
Suitable for MC

Statistical assumption:
any partition of the excitation energy E^* among N, $N = N_h + N_p$, excitons has the same probability to occur
Step: nucleon-nucleon collision with $N_{n+1}=N_n+2$ ("never come back approximation)
Chain end = equilibrium = N_n sufficiently high or excitation energy below threshold

N_1 depends on the reaction type and cascade history

Thin target example

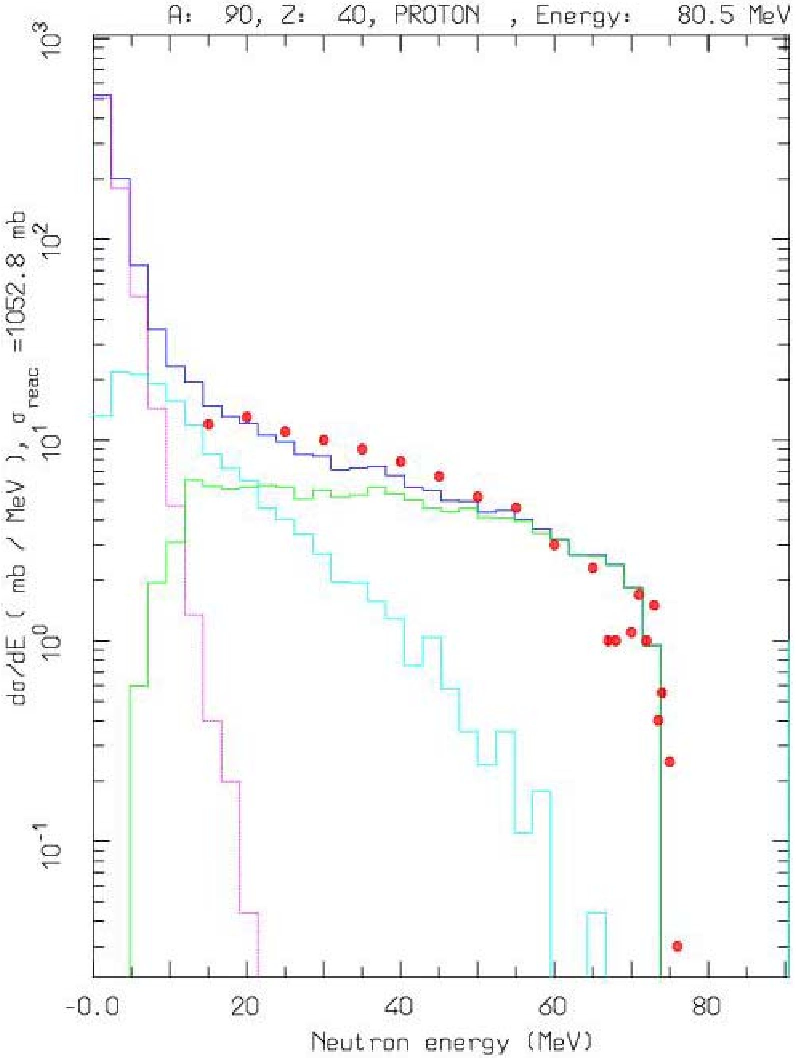

Angle-integrated $^{90}Zr(p,xn)$ at 80.5 MeV

The various lines show the total, INC, preequilibrium and evaporation contributions

Experimental data from
M. Trabandt et al., Phys. Rev. C39, 452 (1989)

Thin target examples: p + ^{80}Zr $\rightarrow$ p + X (80 MeV)

Classical INC

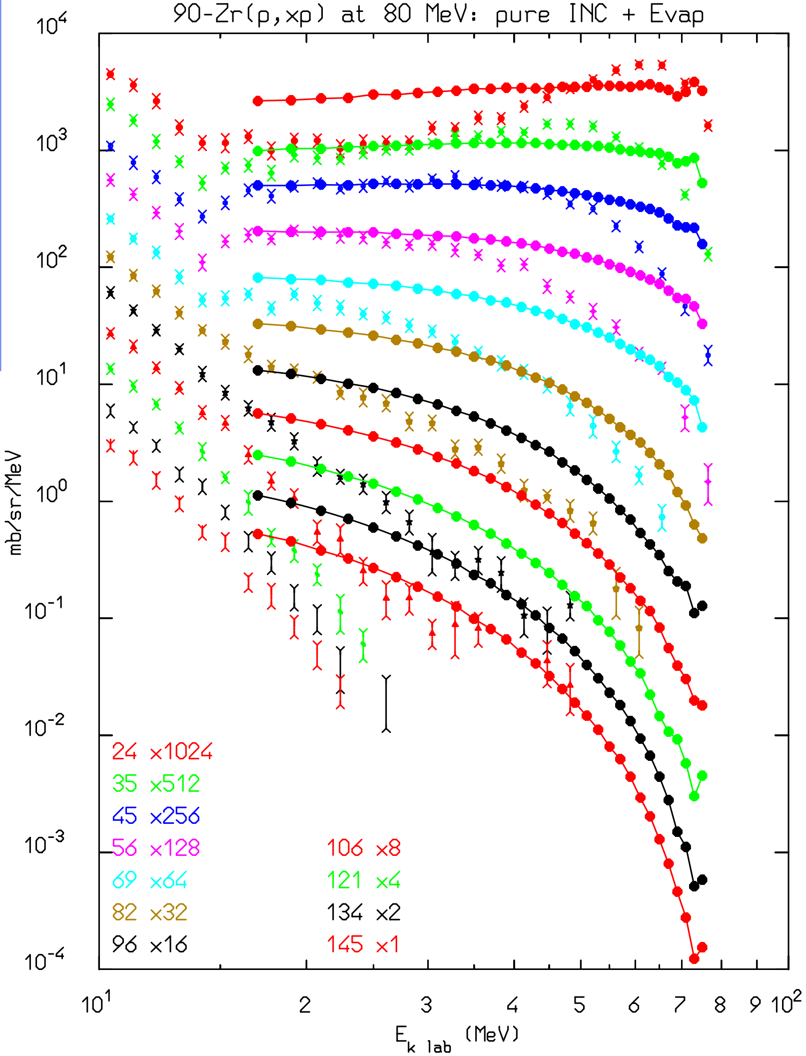

Generalized INC

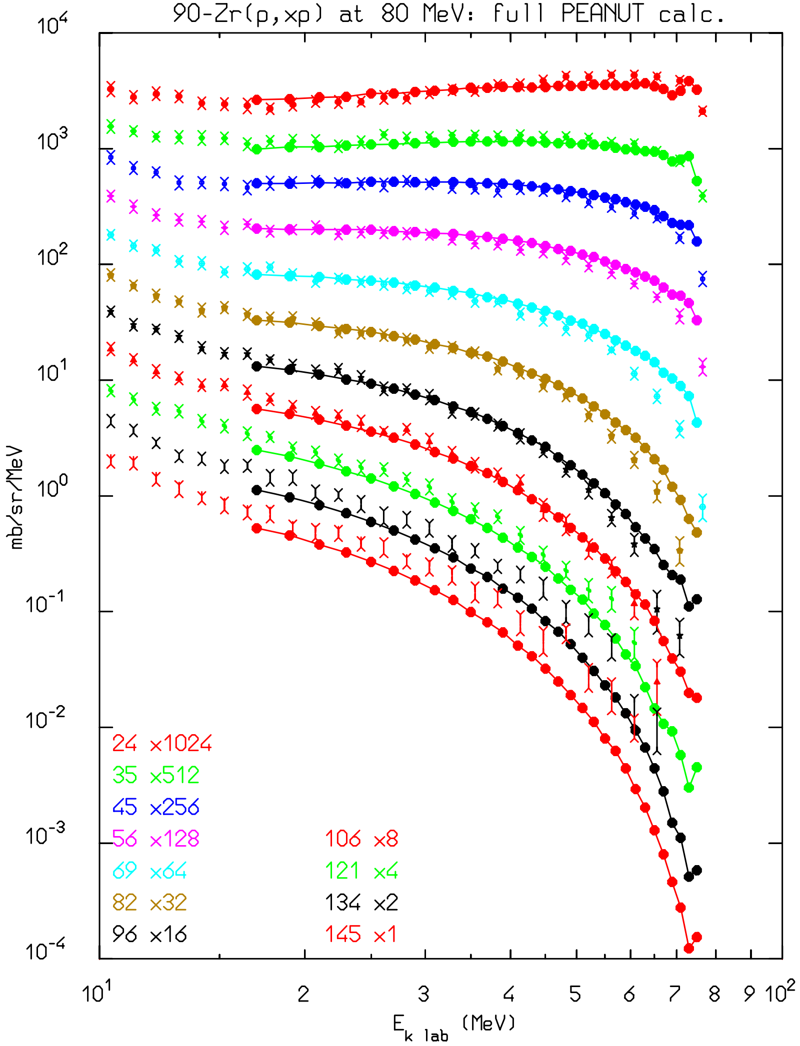

Thick/Thin target examples: neutrons

$^9Be(p,xn)$ @ 256 MeV, stopping target

Data: NSE110, 299 (1992)

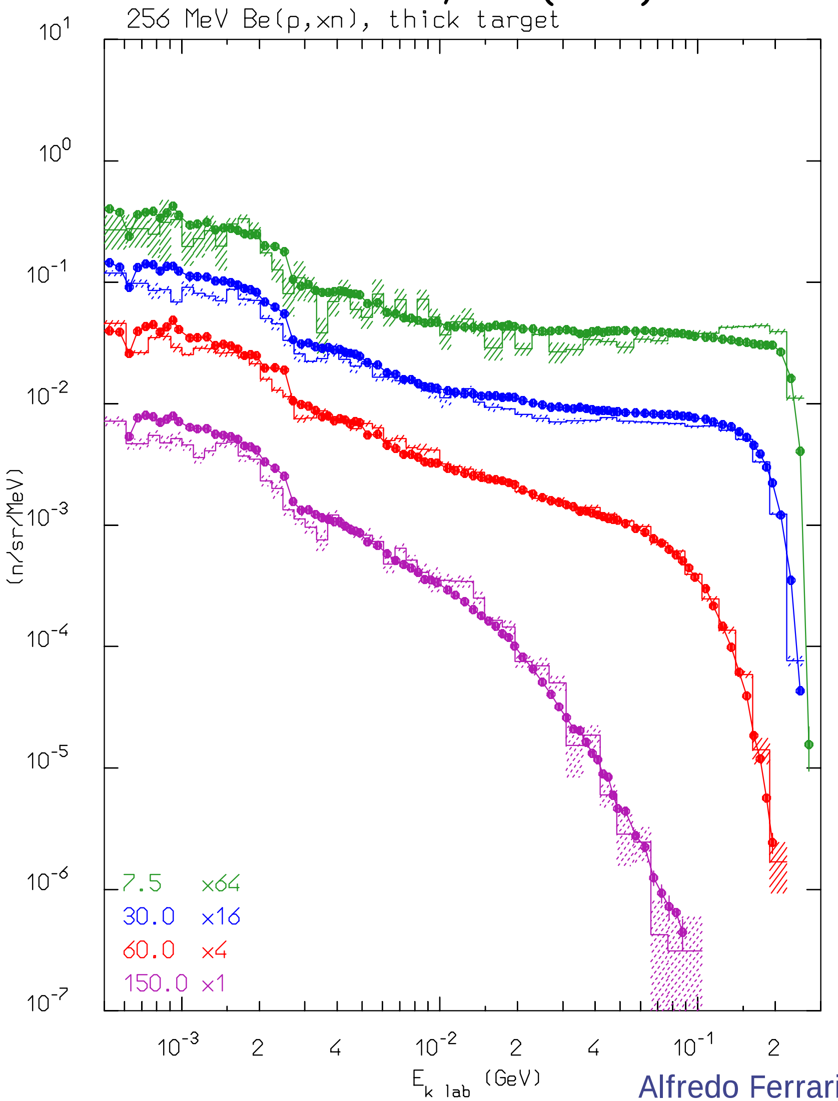

Pb(p,xn) @ 3 GeV, thin target

Data: NST32, 827 (1995)

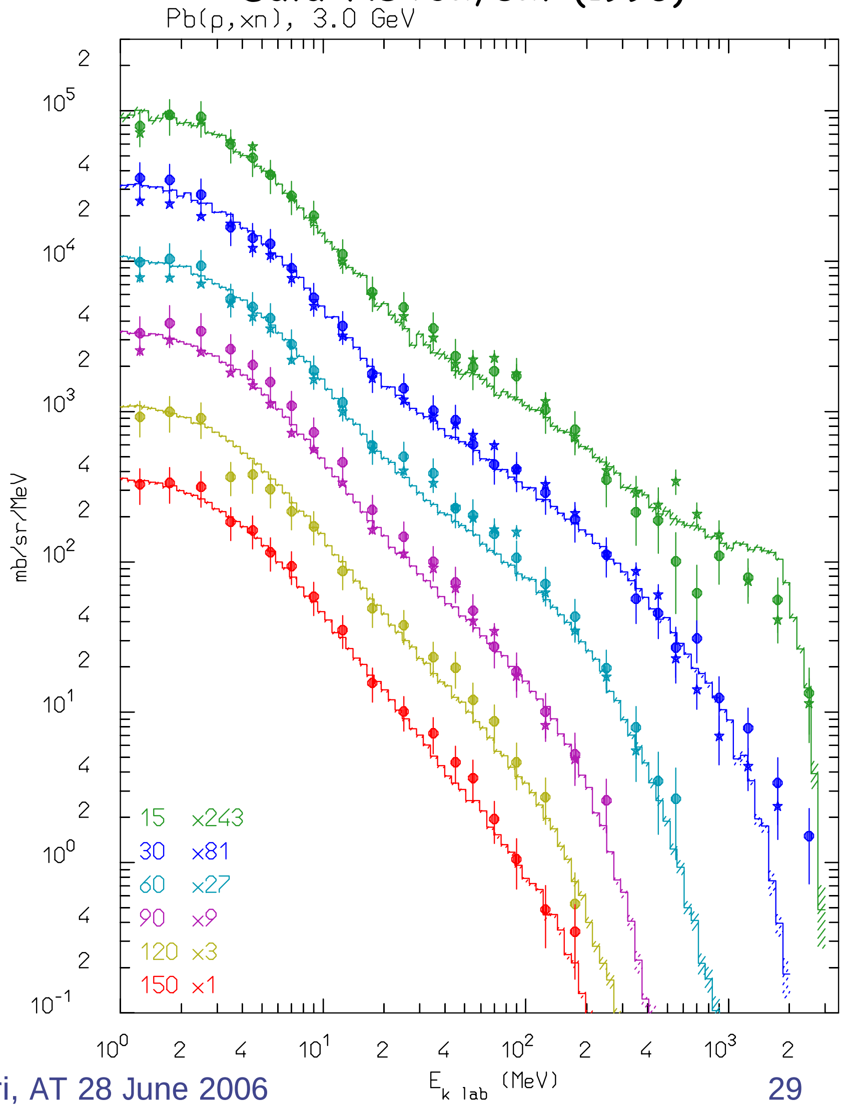

Thin target examples: pions

$\pi^{+/-}$ absorption cross section on Gold and Bismuth

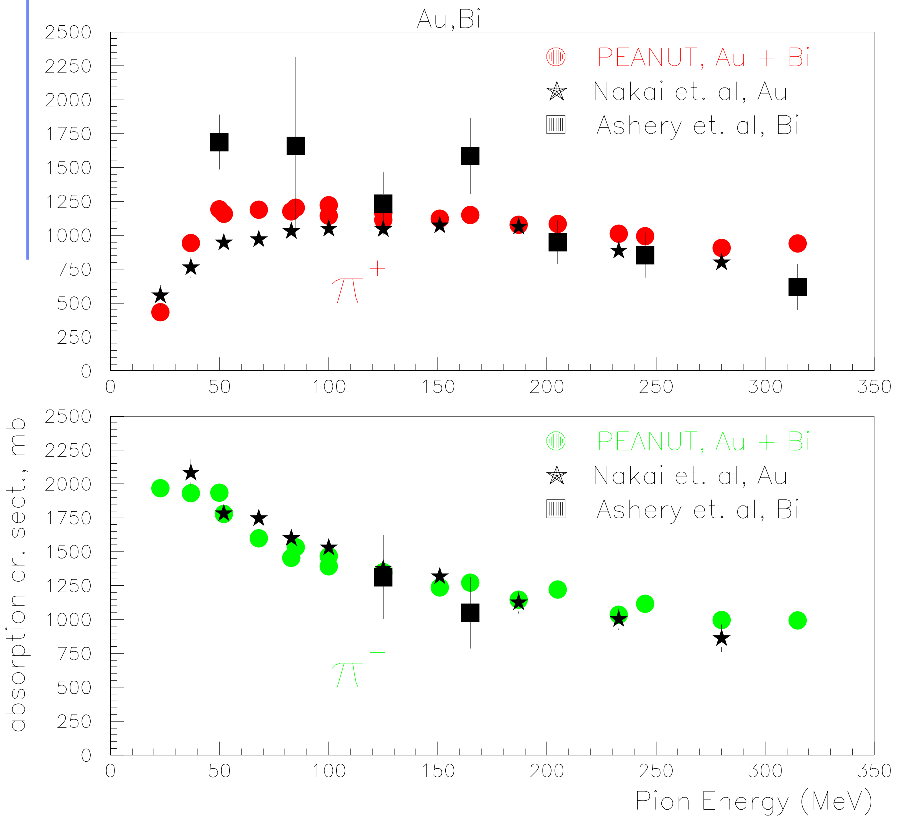

p + Al $\rightarrow \pi^-$ + X (4 GeV/c)

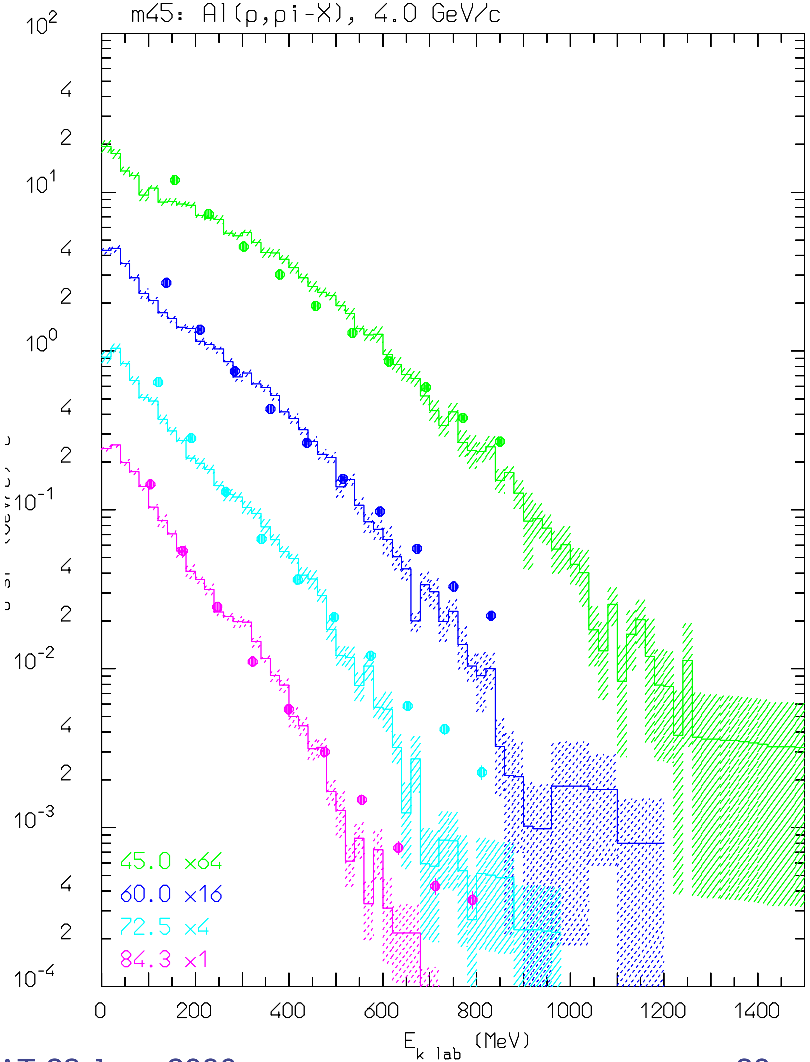

Equilibrium particle emission (evaporation, fission and nuclear break-up)

From statistical considerations and the detailed balance principle, the probabilities for emitting a particle of mass m_j, spin $S_j \hbar$ and energy E, or of fissioning are given by:
(i, f for initial/final state, Fiss for fission saddle point)

Probability per unit time of emitting a particle j with energy E

$$P_J = \frac{(2S_j + 1) m_j c}{\pi^2 \hbar^3} \int_{V_j}^{U_i - Q_j - \Delta_f} \frac{\rho_f (U_f)}{\rho_i (U_i)} \sigma_{inv}(E) E dE$$

Probability per unit time of fissioning

$$P_{Fiss} = \frac{1}{2 \pi \hbar} \int_0^{U_i - B_{Fiss}} \frac{\rho_{Fiss}(U_i - B_{Fiss} - E)}{\rho_i (U_i)} dE$$

- ρ's: nuclear level densities
- U's: excitation energies
- V_j's: possible Coulomb barrier for emitting a particle type j
- B_{Fiss}: fission barrier

- Q_j's: reaction Q for emitting a particle type j
- σ_{inv}: cross section for the inverse process
- Δ's: pairing energies

Neutron emission is strongly favoured because of the lack of any barrier
Heavy nuclei generally reach higher excitations because of more intense cascading

Residual Nuclei

- The production of residuals is the result of the last step of the nuclear reaction, thus it is influenced by all the previous stages
- Residual mass distributions are very well reproduced
- Residuals near to the compound mass are usually well reproduced
- However, the production of specific isotopes may be influenced by additional problems which have little or no impact on the emitted particle spectra (Sensitive to details of evaporation, Nuclear structure effects, Lack of spin-parity dependent calculations in most MC models)

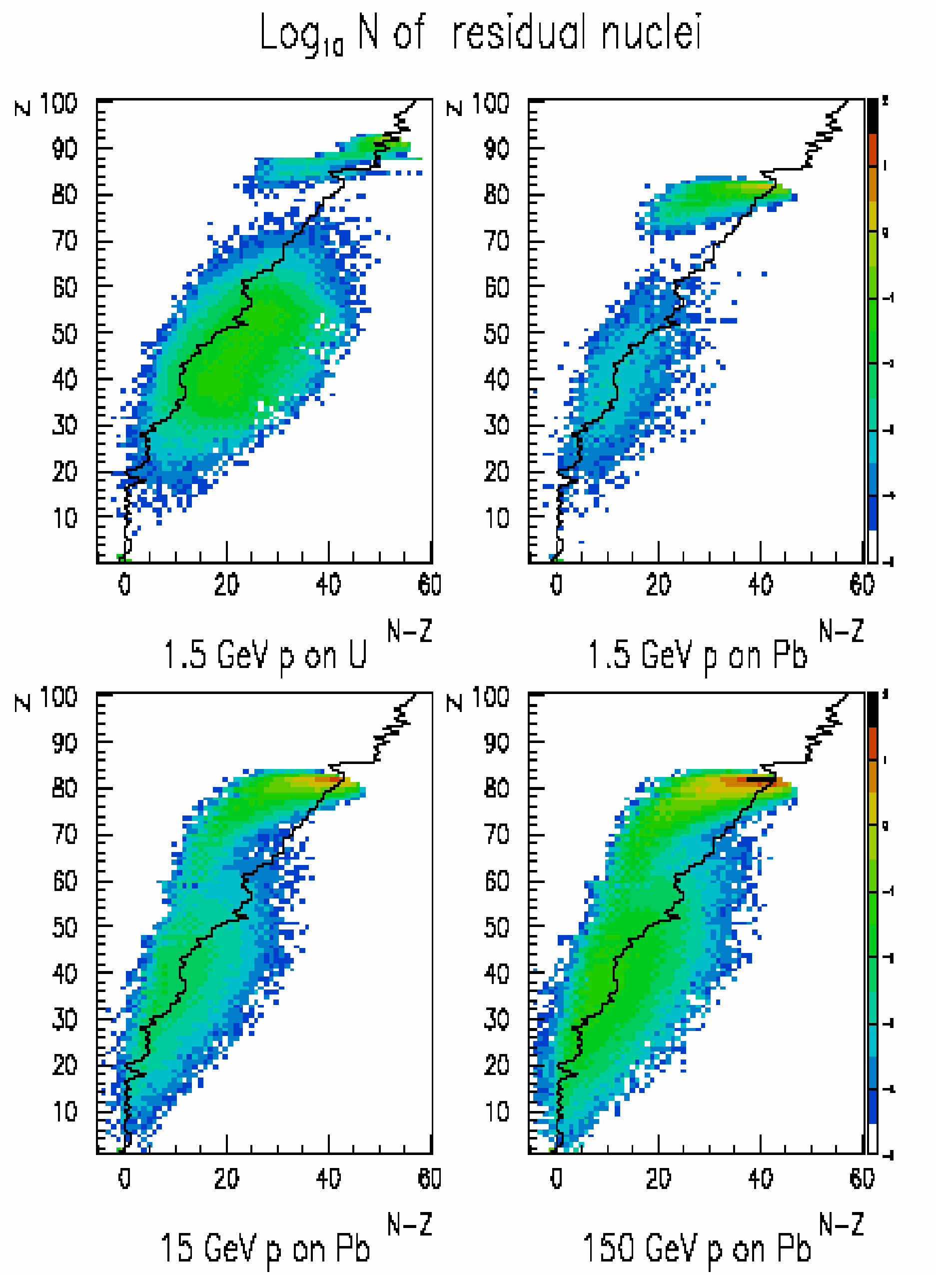

Example of fission/evaporation

- Quasi-elastic products
- Spallation products
- Deep spallation products
- Fission products
- Fragmentation products
- Evaporation products

1 A GeV ^{208}Pb + p reactions Nucl. Phys. A 686 (2001) 481-524

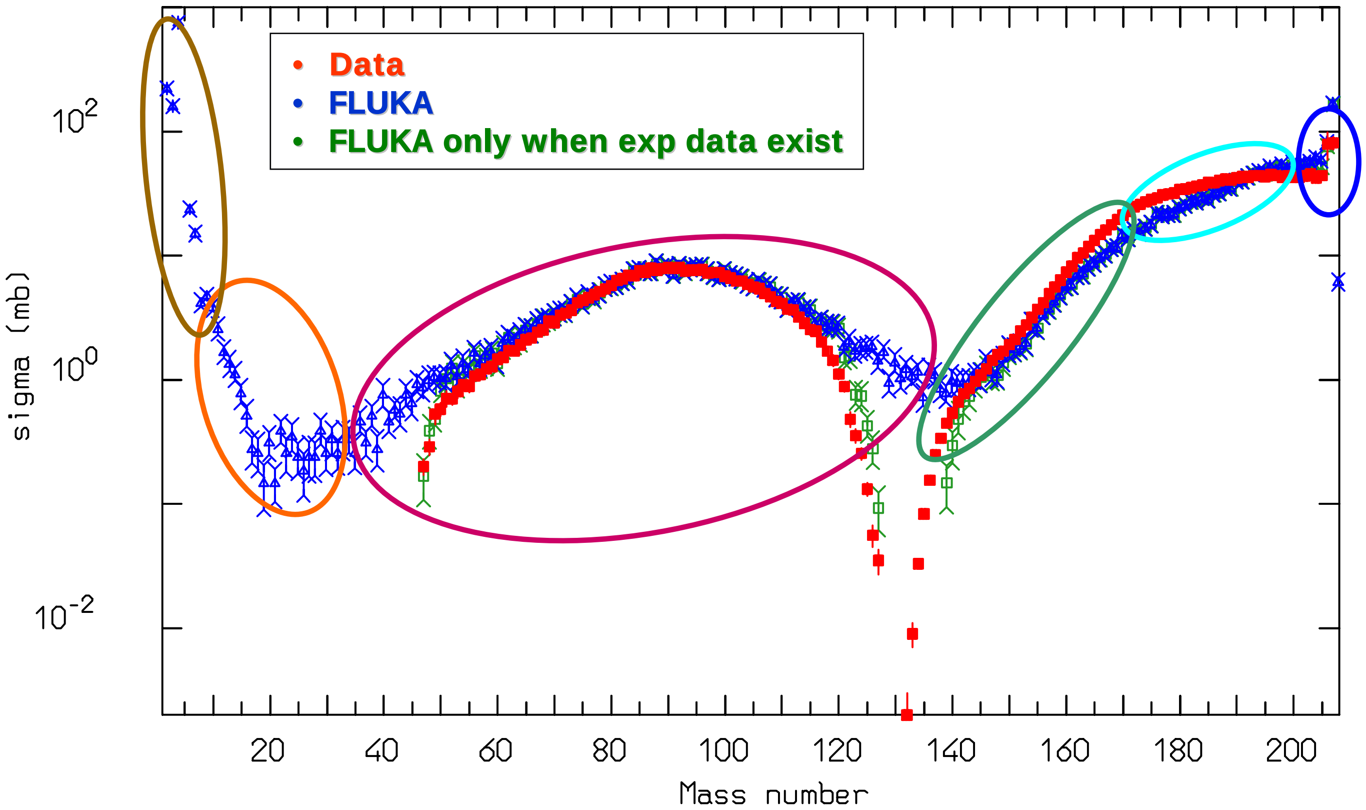

Heavy ion interaction models

Intermediate energy range (~100 MeV/n to a few GeV/n): three main classes of microscopic models suitable for MonteCarlo.

They are microscopic kinetic models including the propagation and mutual interactions of pion and nucleon resonances. Similar two body collision terms mostly based on free scattering

- **(Generalized)IntraNuclear Cascade model**
  - Nuclear mean field
  - Semiclassical trajectories
- **Quantum Molecular Dynamics models**
  - Gaussian packet wave functions for nucleons
  - Nucleon mean field as the sum of two-body potentials
- **BUU (Boltzmann-Uehling-Uhlenbeck) eq. based models**
  - Time evolution equation of the nucleon (pions...), one-body phase-space distribution
  - Test particle method (semiclassical trajectories in a self-consistent mean field)

(G)INC and QMD models successfully extended up to very high energies and all hadrons with Glauber + string models (like DPM)

FLUKA with modified RQMD-2.4

(Projectile) fragmentation is the name of the game for heavy ion interactions

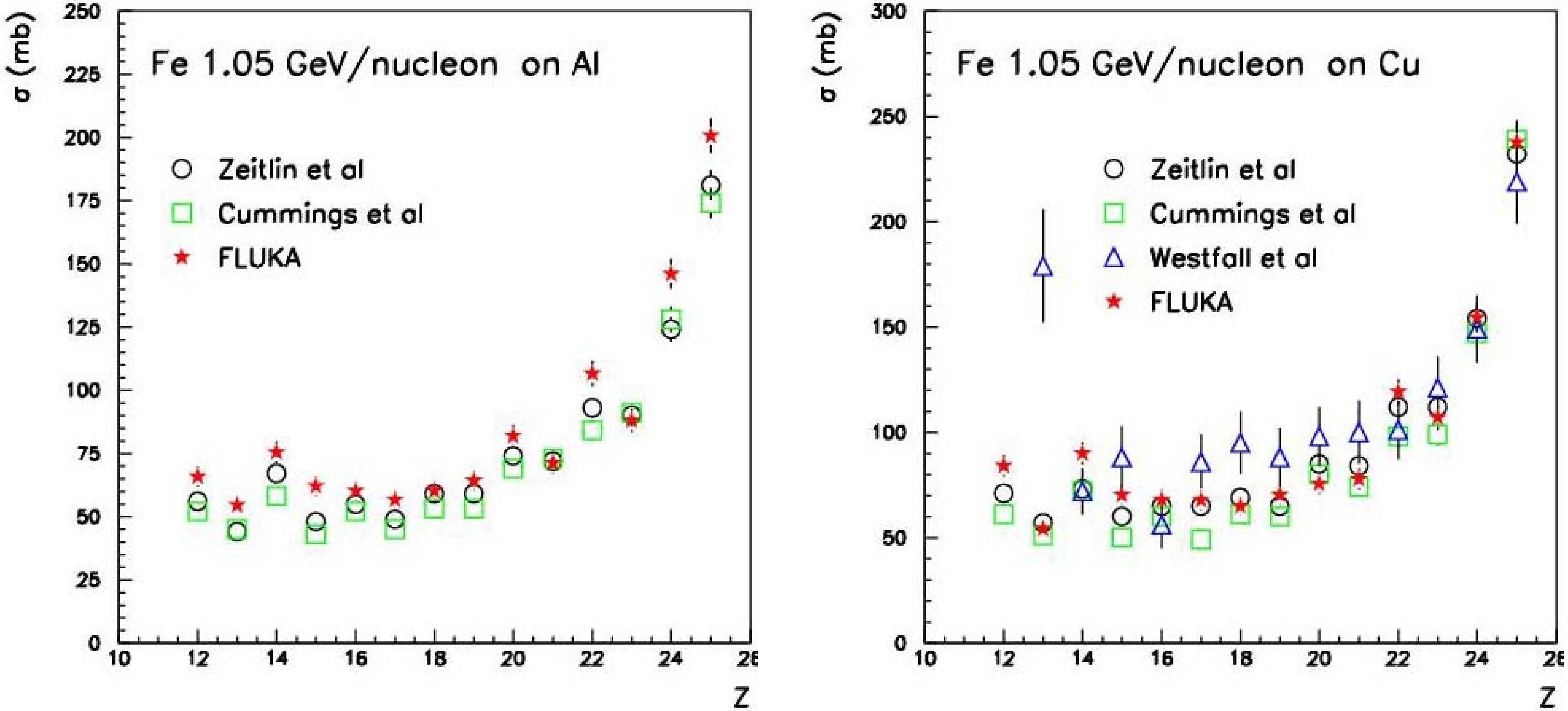

Fragment charge cross section for 1.05 GeV/n Fe ions on Al (left) and Cu (right). ★: FLUKA, ○ : PRC 56, 388 (1997), □ : PRC42, 5208 (1990), Δ: PRC 19, 1309 (1979)

FLUKA fragmentation results

Fragment charge cross section for 750 MeV/n U ions on Pb.

Data (stars) from

J. Benlliure, P. Ambruster et al., Eur. Phys. J. A2, 193-198 (1988).

Fission products have been excluded like in the experimental analysis

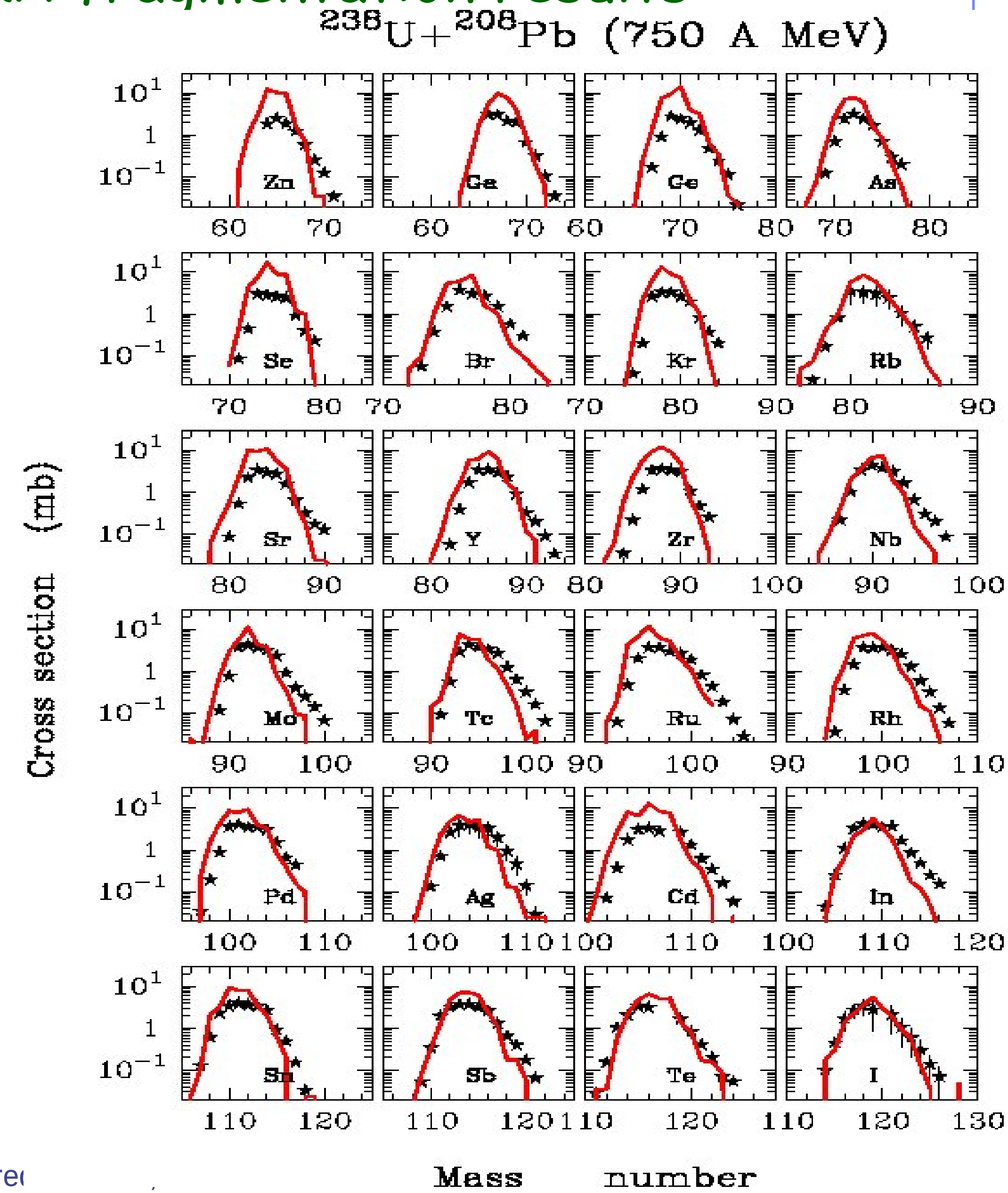

FLUKA with modified RQMD-2.4

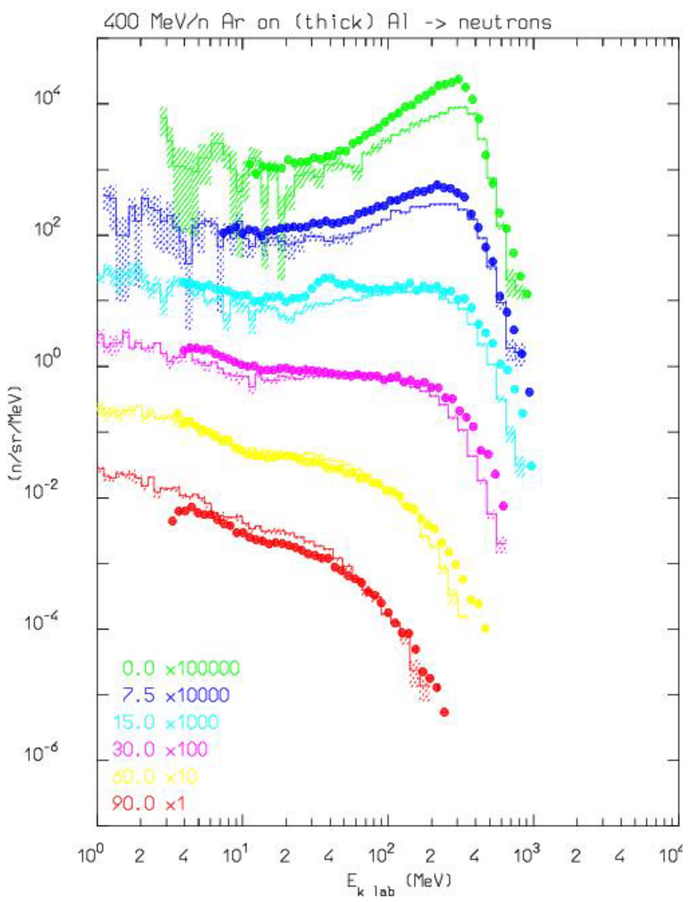

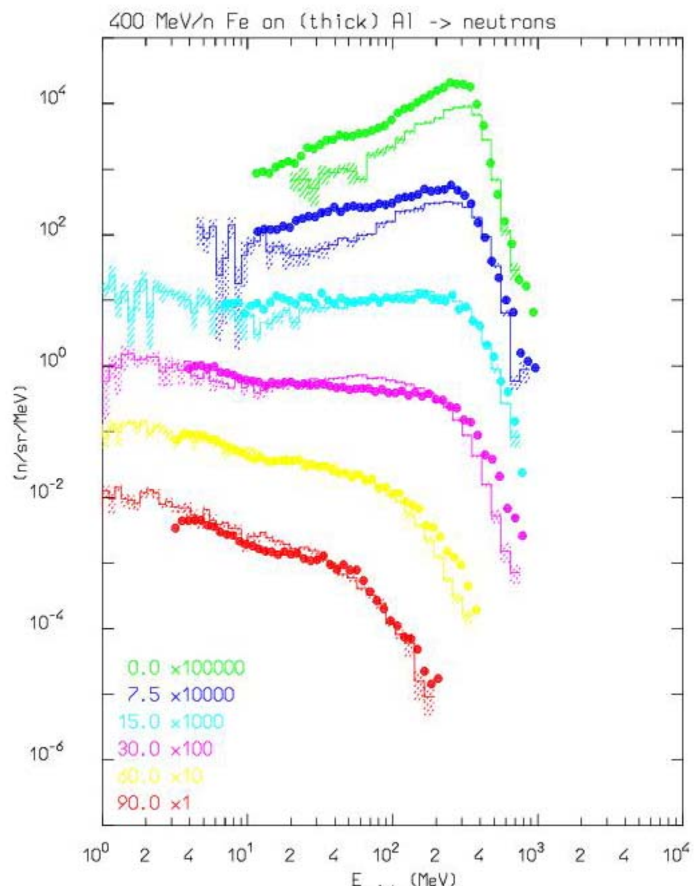

Double-differential neutron yield by 400 MeV/n Ar (left) and Fe (right) ions on thick Al targets. Histogram: FLUKA. Experimental data points: Phys. Rev. C62, 044615 (2000)

Ar + Al double differential neutron production cross - section

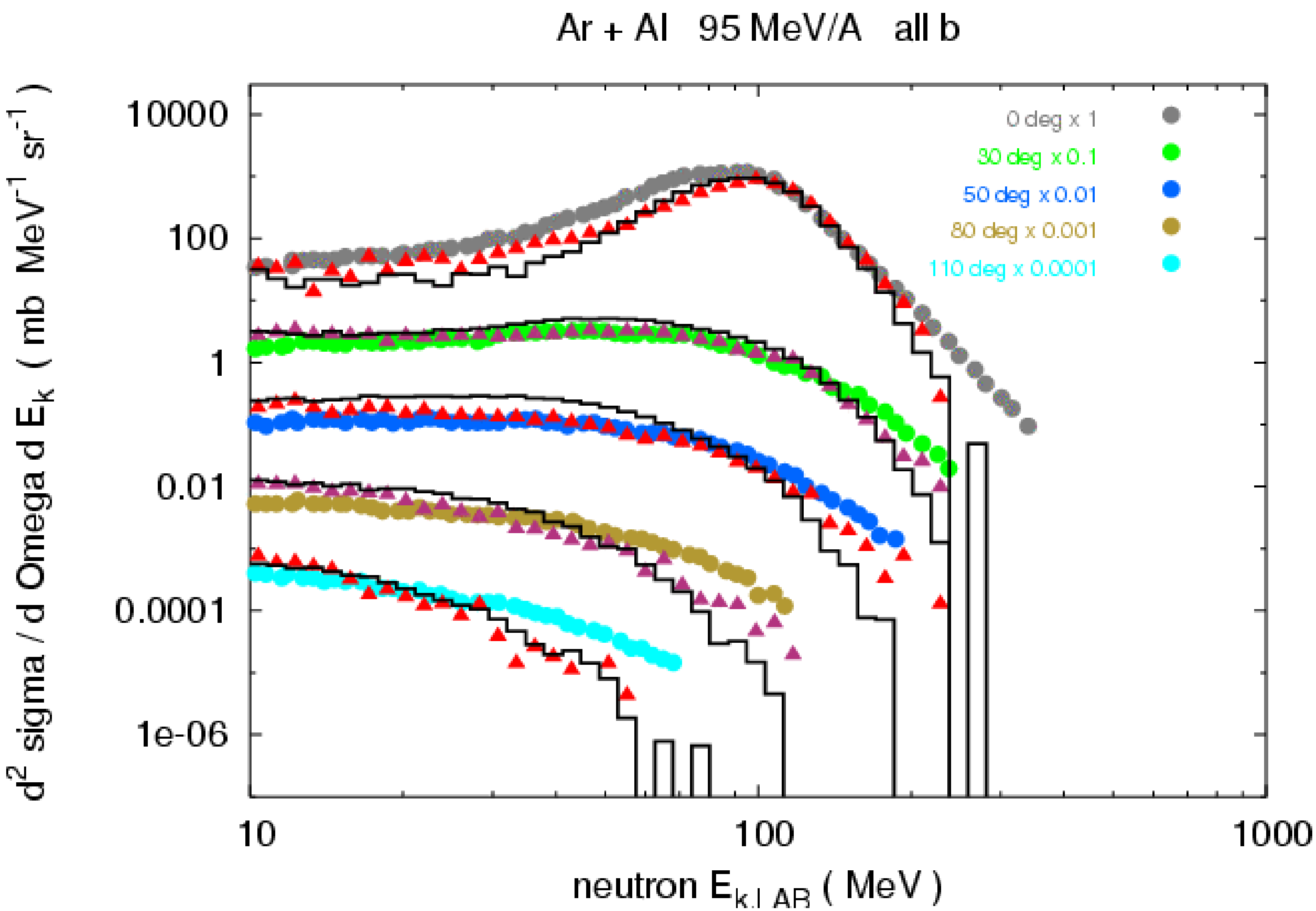

RQMD + FLUKA ▲ QMD + FLUKA ● EXP data

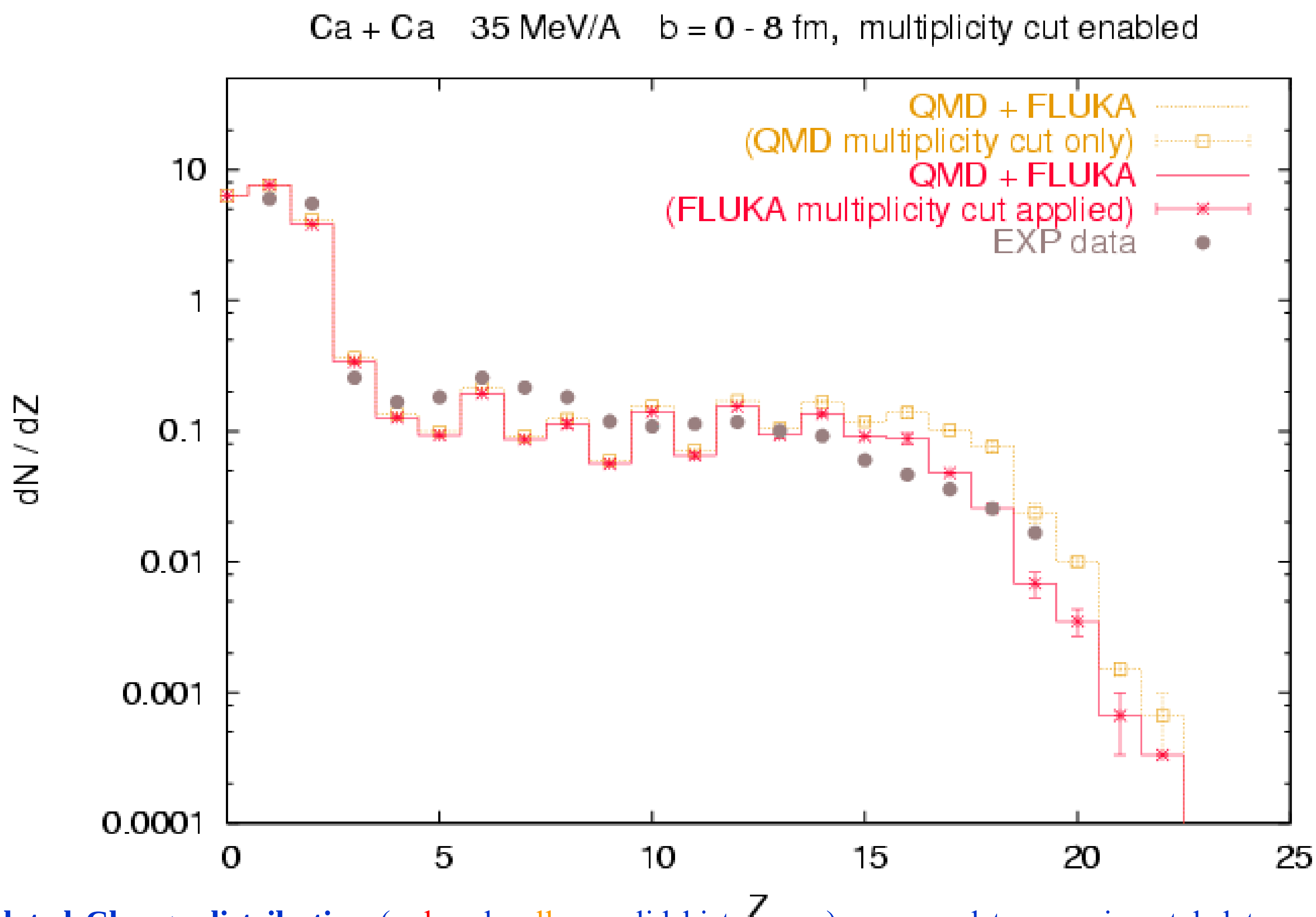

Simulated Charge distribution (red and yellow solid histograms) compared to experimental data collected in central collisions (grey points) by the AMPHORA detector at SARA. The simulation results are **sensitive to the experimental cuts**, as can be seen comparing the yellow line, obtained imposing a multiplicity cut of $M_z > 5$ at the end of the fast stage of the reaction, described by QMD, to the red line, obtained adding at the end of the interaction a multiplicity cut of $M_z > 10$ and the requirements of quasicomplete events taking into account the acceptance of the detector.

Real and Virtual Photonuclear Interactions

Photonuclear reactions

- Giant Dipole Resonance interaction (special database)
- Quasi-Deuteron effect
- Delta Resonance energy region
- Vector Meson Dominance in the high energy region
- (G)INC, preequilibrium and evaporation like for hadron-nucleus

Virtual photon reactions

- Muon photonuclear interactions
- Electromagnetic dissociation

Photonuclear int.: example

Reaction:
$^{208}Pb(\gamma,x\ n)$
$20 \leq E\gamma \leq 140$ MeV

Cross section for multiple neutron emission as a function of photon energy, Different colors refer to neutron multiplicity $\geq n$, with $2 \leq n \leq 8$

Symbols: exp data (NPA367, 237 (1981) ; NPA390, 221 (1982))

Lines: FLUKA

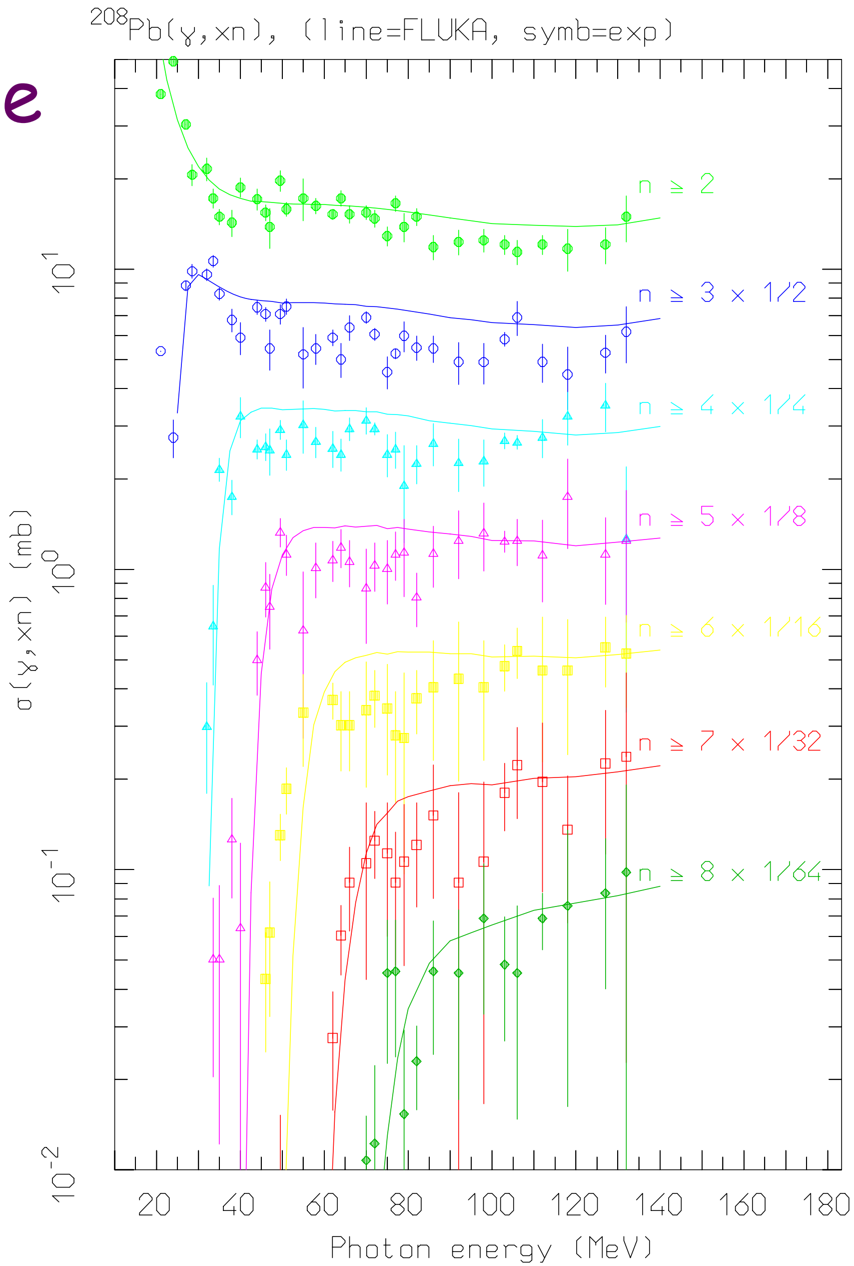

Electromagnetic dissociation

Electromagnetic dissociation: σ_{EM} increasingly large with (target) Z's and energy. Already relevant for few GeV/n ions on heavy targets (σ_{EM} ~ 1 b vs σ_{nucl} ~ 5 b for 1 GeV/n Fe on Pb)

$$\sigma_{1\gamma} = \int \frac{d\omega}{\omega} n_{A_1}(\omega)\sigma_\gamma n_{A_2}(\omega) \propto Z_1^2$$

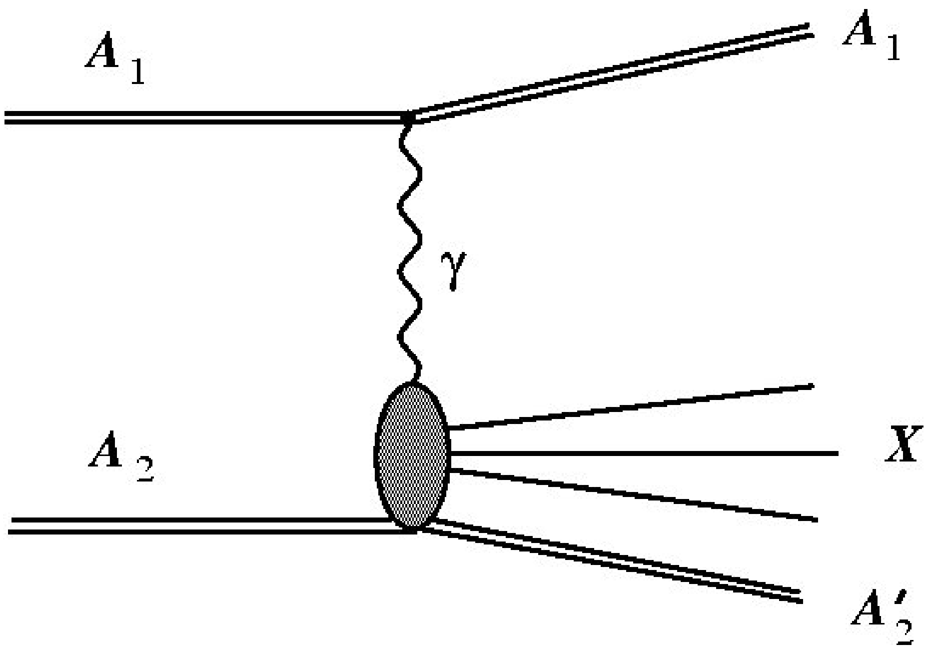

Electromagnetic dissociation: example

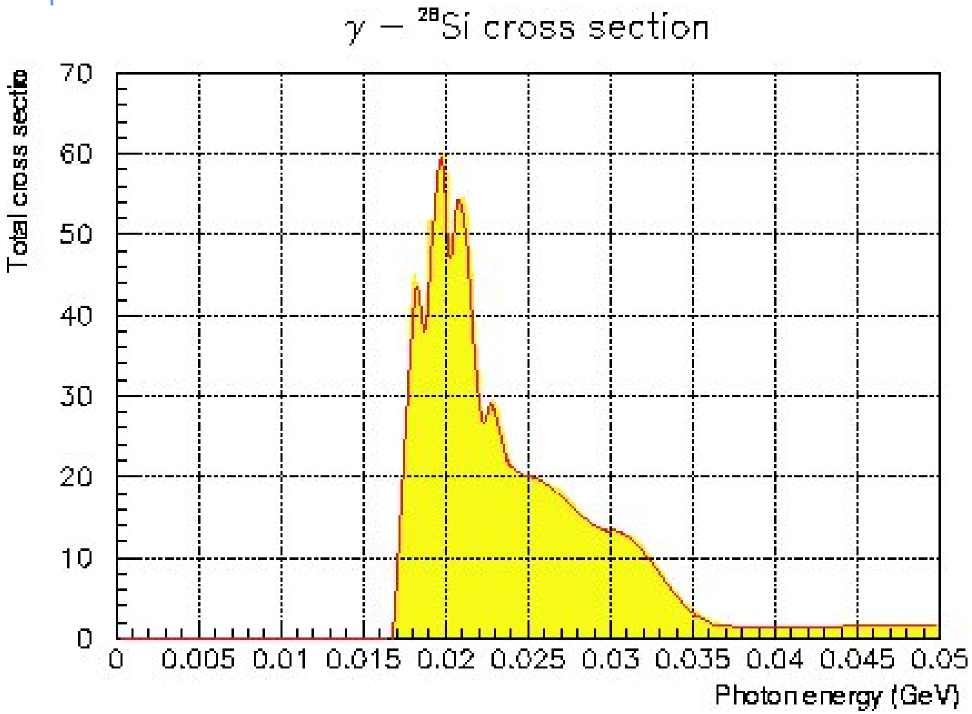

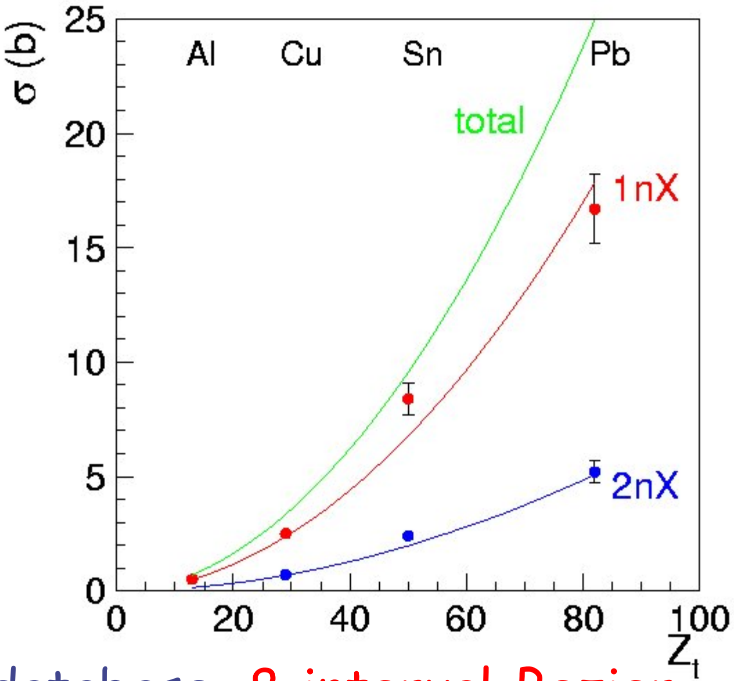

Left: ^{28}Si(g,tot) as recorded in FLUKA database, 8 interval Bezier fit as used for the Electromagnetic Dissociation event generator.

Right: calculated total, 1nX and 2nX electromagnetic dissociation cross sections for 30 A GeV Pb ions on Al, Cu, Sn and Pb targets. Points – measured cross sections of forward 1n and 2n emissions as a function of target charge (M.B. Golubeva et al., in press)

158 GeV/n fragmentation

Fragment charge cross section for 158 AGeV Pb ions on various targets. Data (symbols) from NPA662, 207 (2000), NPA707, 513 (2002) (blue circles) and from C.Scheidenberger et al. PRC, in press (red squares), histos are FLUKA (with DPMJET-III) predictions: the dashed histo is the electromagnetic dissociation contribution

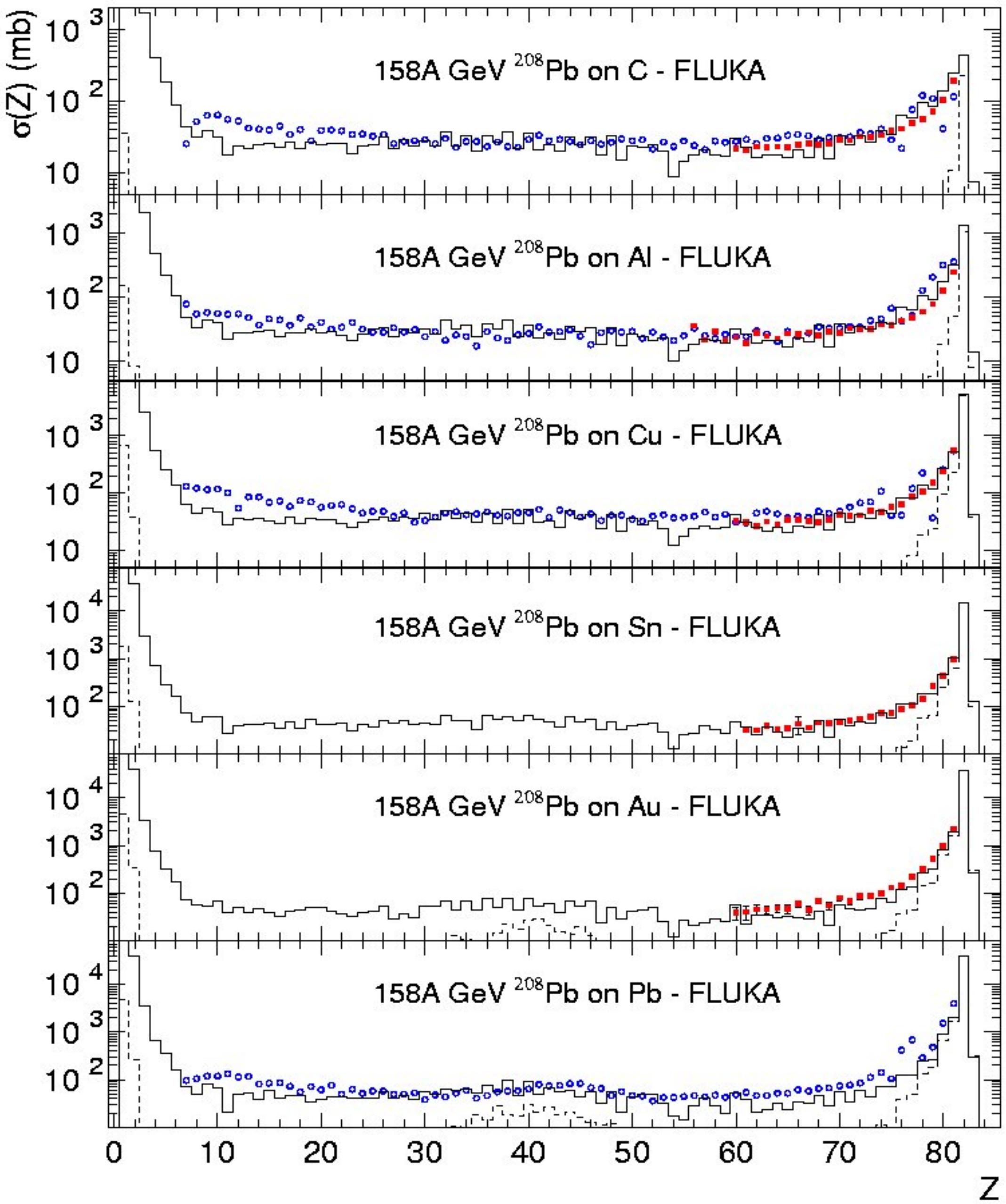

Examples of Applications

CERN-EU High-Energy Reference Field (CERF) facility

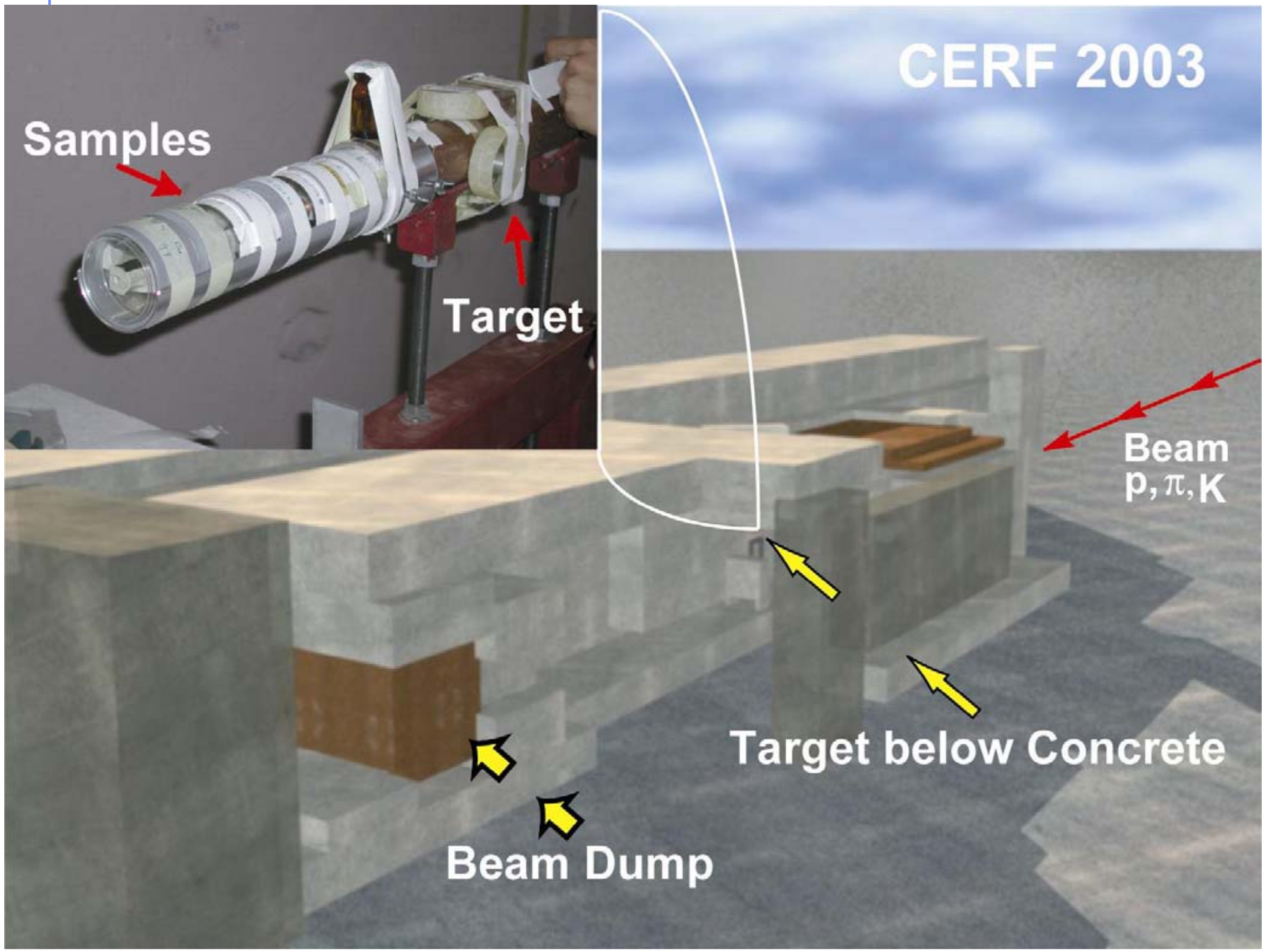

Location of Samples:

Behind a 50 cm long, 7 cm diameter copper target, centred with the beam axis

Calculation of Induced Activity with FLUKA

- Simulation of particle interactions and transport in the target, the samples, as well as the tunnel/cavern walls
- Separate simulations for proton and pion beam
- Simulations of isotope production via
  - High-energy processes
  - Low-energy neutron interactions
- Transport thresholds
  - Neutrons: down to thermal energies
  - Other hadrons: until stopped or captured
  - No electromagnetic cascade was simulated
- Calculated quantities
  - Radioactive isotope production per primary particle
  - (Star density and particle energy spectra in the samples)
- Calculation of build-up and decay of radioactive isotopes for specific irradiation and cooling patterns including radioactive daughter products

Activation: Stainless Steel

Table 1: Stainless Steel, cooling times 1d 6h 28m, 17d 10h 39m

Isotope	$t_{1/2}$	Exp Bq/g	± %	OLD FLUKA/Exp	± %	FLUKA/Exp	± %
Be 7	53.29d	0.205	24	0.096	34	1.070	30
Na 24	14.96h	0.513	4.3	0.278	8.6	0.406	13
K 43	22.30h	1.08	4.6	0.628	8.7	0.814	11
Ca 47	4.54d	0.098	25	0.424	44	(0.295	62)
Sc 44	3.93h	13.8	4.8	0.692	5.8	0.622	6.2
mSc 44	58.60h	6.51	7.1	1.372	8.1	1.233	8.6
Sc 46	83.79d	0.873	8.3	0.841	9.1	0.859	9.5
Sc 47	80.28h	6.57	8.2	0.970	9.7	1.050	13
Sc 48	43.67h	1.57	5.2	1.266	8.4	1.403	11
V 48	15.97d	8.97	3.1	1.464	3.8	1.354	4.8
Cr 48	21.56h	0.584	6.7	1.084	11	1.032	12
Cr 51	27.70d	15.1	12	1.261	13	1.231	13
Mn 54	312.12d	2.85	10	1.061	10	1.060	11
Co 55	17.53h	1.04	4.6	1.112	7.7	0.980	10
Co 56	77.27d	0.485	7.6	1.422	9.0	1.332	10
Co 57	271.79d	0.463	11	1.180	12	1.140	12
Co 58	70.82d	2.21	5.9	0.930	6.3	0.881	6.9
Ni 57	35.60h	3.52	4.5	1.477	6.5	1.412	8.2

M. Brugger, *et al.*, Proceedings of the Int. Conf. on Accelerator Applications (AccApp'05), Venice, Italy, 2005

Activation: Aluminum

Table 2: Al, cooling times 1d 16h, 16d 08h , 51d 09h

Isotope	$t_{1/2}$	Exp Bq/g	± %	OLD FLUKA/Exp	± %	FLUKA/Exp	± %
Be 7	53.29d	0.789	13	0.364	16	0.688	19
Na 22	2.60y	0.365	9.6	0.841	11	0.752	11
Na 24	14.96h	38.6	3.6	0.854	4.0	0.815	4.6
Sc 44	3.93h	0.229	24	2.219	27	0.820	36
Sc 46	83.79d	0.025	16	1.571	19	0.902	28
Sc 47	80.28h	0.163	12	0.986	27	(1.486	43)
V 48	15.97d	0.199	7.4	0.931	18	(0.938	29)
Cr 51	27.70d	0.257	17	0.873	23	0.942	28
Mn 52	5.59d	0.224	5.6	2.369	9.6	0.936	24
Mn 54	312.12d	0.081	11	0.972	15	0.917	19
Co 57	271.79d	0.00424	32	0.833	50	(0.760	67)
Co 58	70.82d	0.019	22	1.820	27	0.841	39

M. Brugger, *et al.*, Proceedings of the Int. Conf. on Accelerator Applications (AccApp'05), Venice, Italy, 2005

LHC: Conclusions on activation study

- Good agreement was found between the measured and calculated values for most of the isotopes and samples
- The large number of samples and variety of different materials offers a extensive possibility to study isotope production
- Multifragmentation (**NOW DEVELOPED AND PRESENTED AT INT. CONF. ON NUCLEAR DATA FOR SCIENCE AND TECHN. (Santa Fe 2004)**) has significantly improved the agreement for intermediate and small mass isotopes
- As a consequence, the calculation of remanent dose rates based on an explicit simulation of isotope production and transport of radiation from radioactive decay with FLUKA should also give reliable results → Part 2

Part 2: Radioactivity Produced in LHC Materials: Residual Dose Rates

- Levels of residual dose rates are an important design criterion for any high energy facility
- Residual dose rates for arbitrary locations and cooling times are so far predicted with a rather poor accuracy
  - typically based on the concept of so-called ω-factors and comprising several severe restrictions
  - layouts and material composition of beam-line components and surrounding equipment are often very complex
- Anapproach based on the explicit generation and transport of gamma and beta radiation from radioactive decay should result in much more accurate results

Benchmark experiment – *Results 1*

M. Brugger *et al.,* Radiat. Prot. Dosim. 116 (2005) 12-15

Dose rate as function of cooling time
for different distances between sample and detector

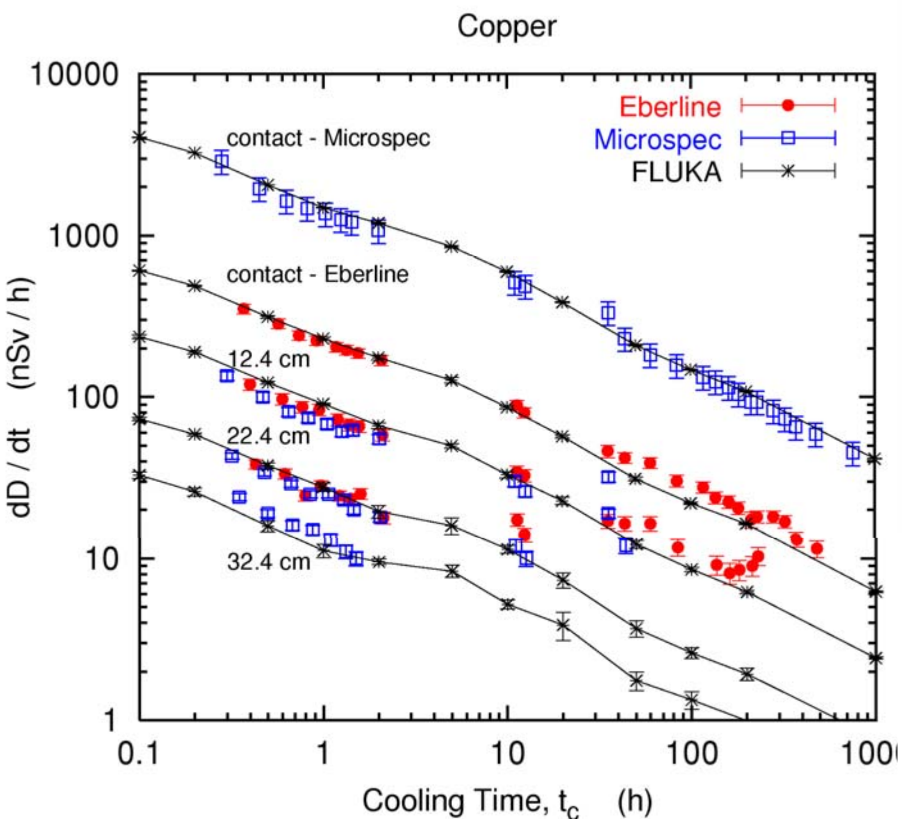

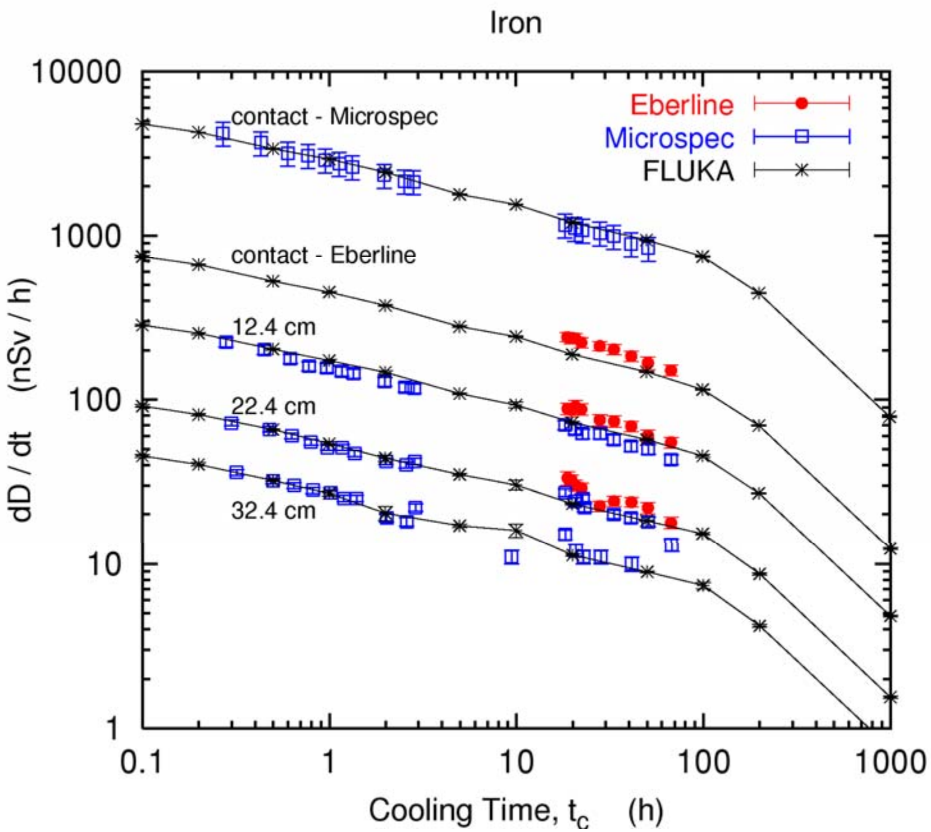

Benchmark experiment – *Results 2*

M. Brugger *et al.*, Radiat. Prot. Dosim. 116 (2005) 12-15

Dose rate as function of cooling time
for different distances between sample and detector

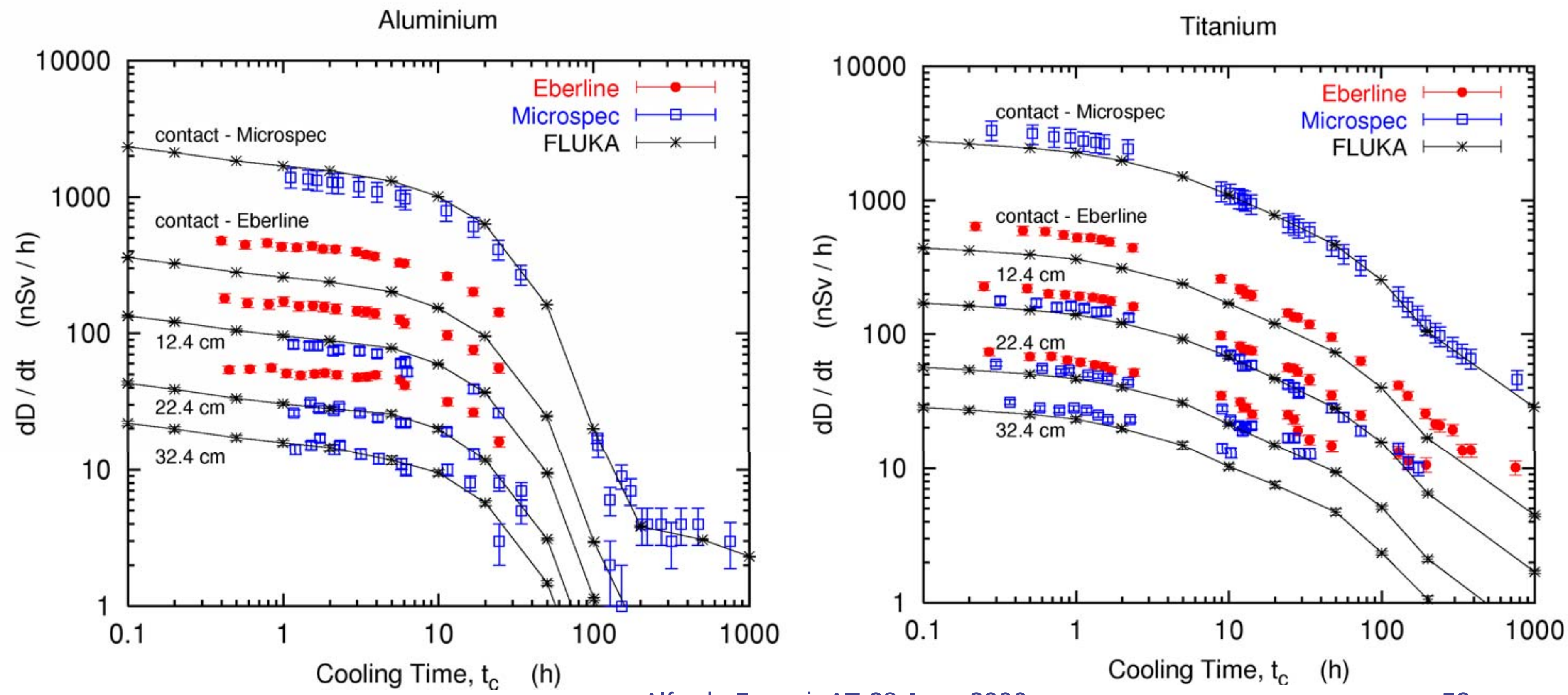

Cosmic Rays

Cosmic Ray physics: Atmospheric Showers, and Space missions

Three different streams:

- Basic research on Cosmic Ray physics (muons, neutrinos, EAS, underground physics,...)
- Application to dosimetry in civil aviation (DOSMAX Collaboration: Dosimetry of Aircrew Exposure to Radiation During Solar Maximum, research project funded by the EU)
- Application to Space missions, in particular manned missions to MARS

Special add-ons required, including:

- Primary spectra from Z = 1 to Z = 28 (derived from NASA and updated to most recent measurements.)
- Solar Modulation model (correlated to neutron monitors)
- Atmospheric model (MSIS Mass-Spectrometer-Incoherent-Scatter)
- 3D geometry of Earth + atmosphere
- Geomagnetic model

(3D) Calculation of Atmospheric ν Flux

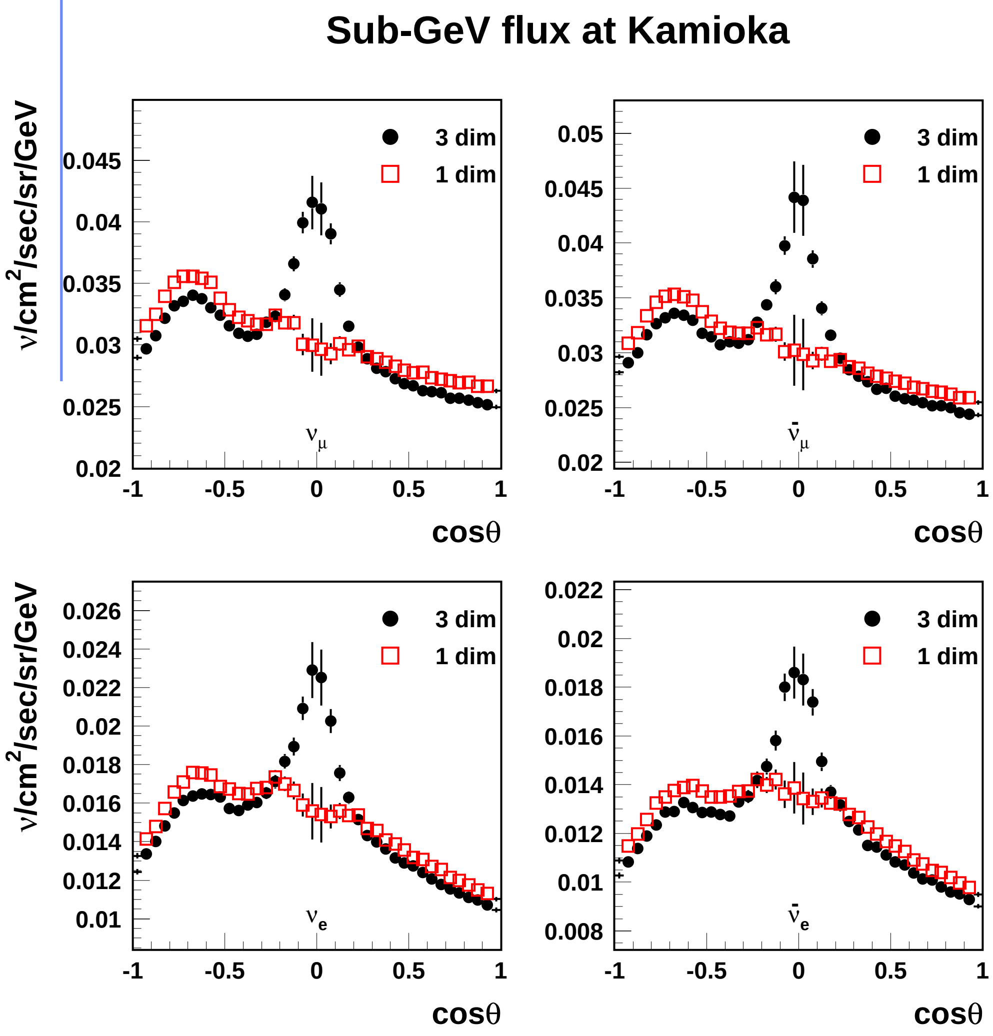

The first 3-D calculation of atmospheric neutrinos was done with FLUKA.

The enhancement in the horizontal direction, which cannot be predicted by a 1-D calculation, was fully unexpected, but is now generally acknowledged.

In the figure: angular distribution of ν_μ, $\bar{\nu}_\mu$, ν_e, $\bar{\nu}_e$.

In red: 1-D calculation

Negative muons at floating altitudes: CAPRICE94

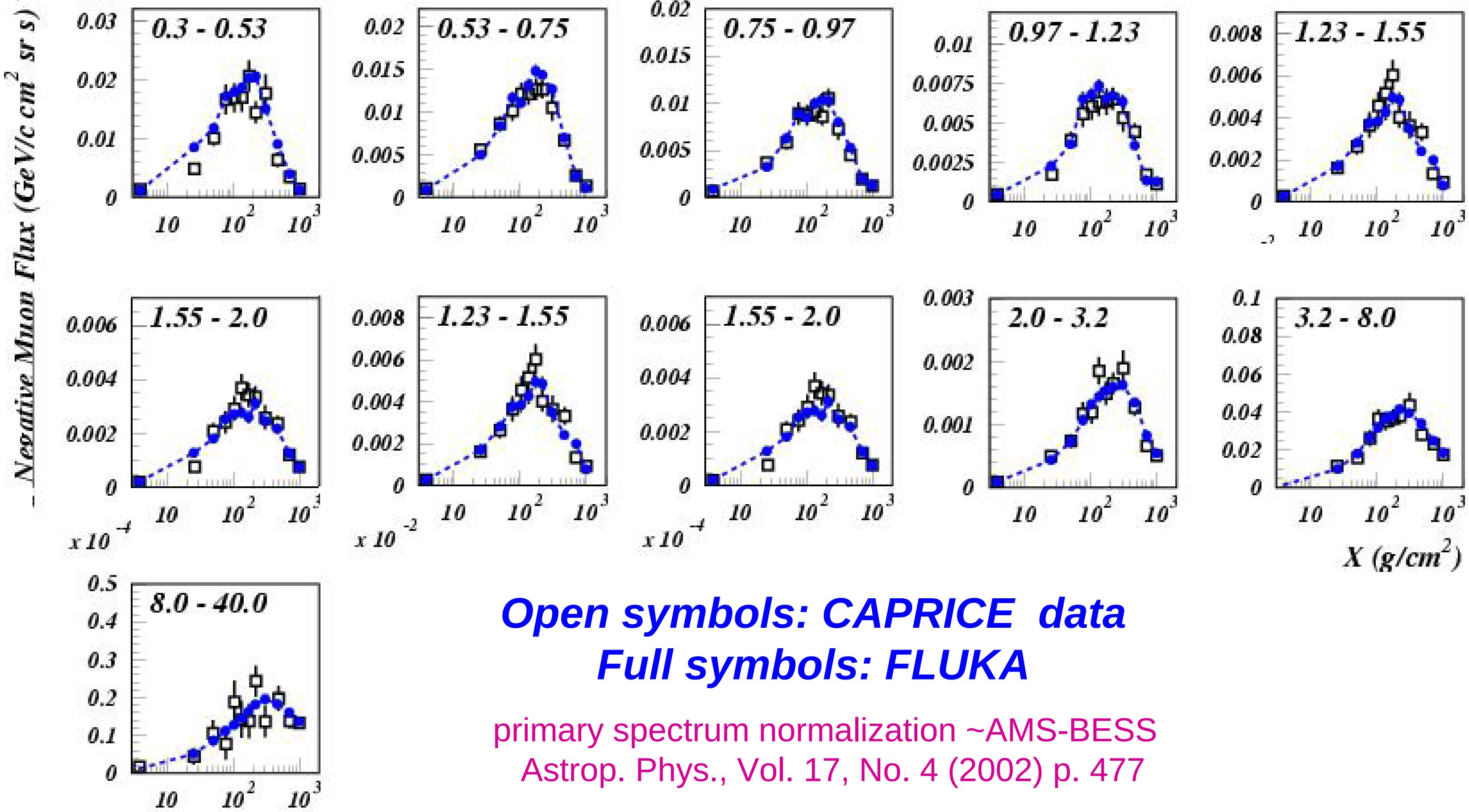

Open symbols: CAPRICE data
Full symbols: FLUKA

primary spectrum normalization ~AMS-BESS
Astrop. Phys., Vol. 17, No. 4 (2002) p. 477

Neutrons on the ER-2 plane at 21 km altitude

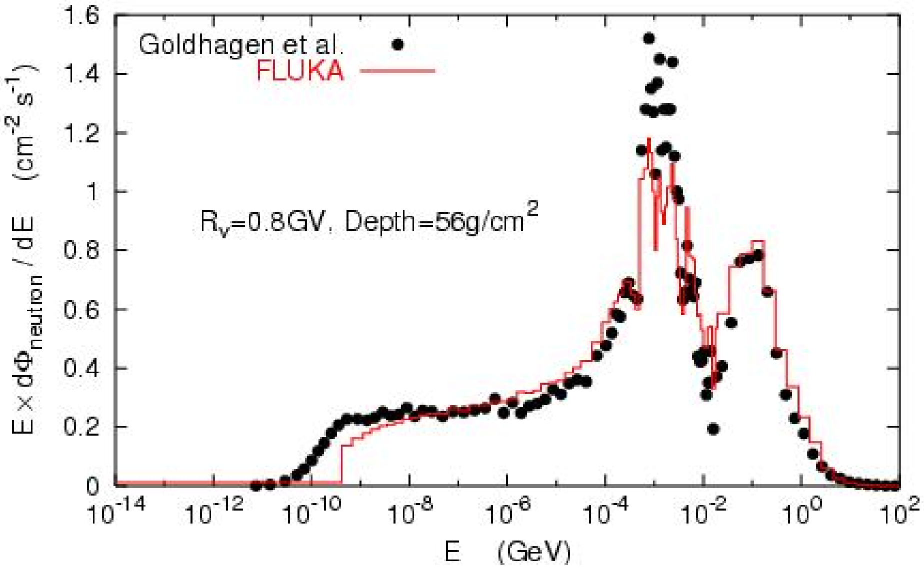

Measurements:

Goldhagen et al., NIM A476, 42 (2002)

Note one order of magnitude difference depending on latitude

FLUKA calculations:

Roesler et al., Rad. Prot. Dosim. 98, 367 (2002)

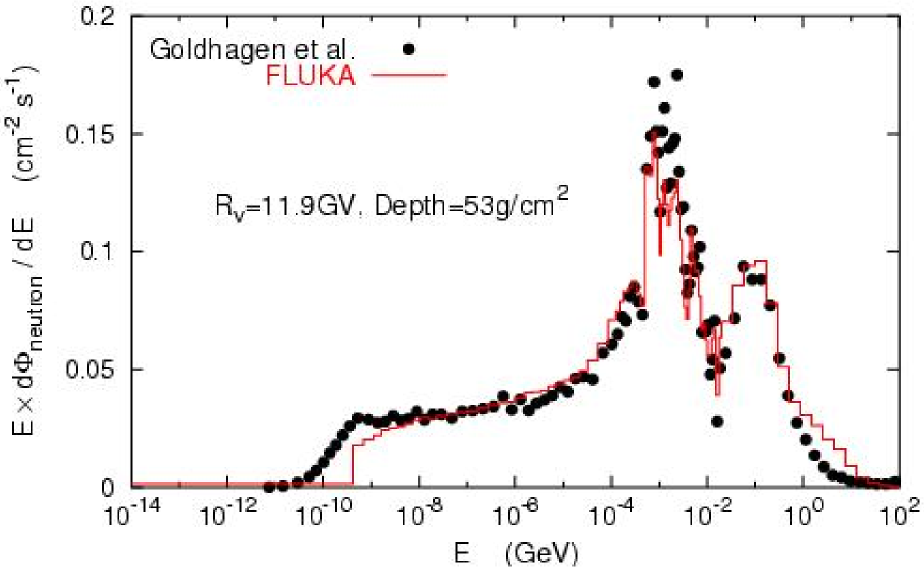

Dosimetry Applications

Roesler et al.,
Rad. Prot. Dosim.
98, 367 (2002)

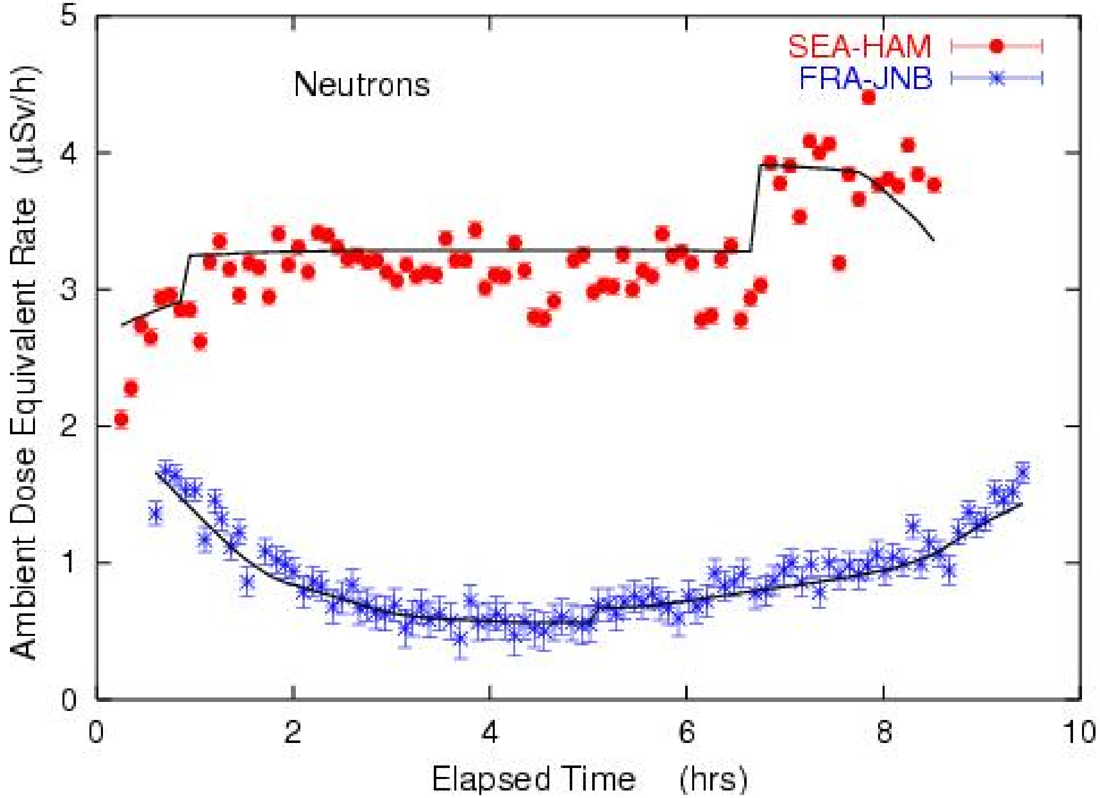

Ambient dose equivalent from neutrons at solar maximum on commercial flights from Seattle to Hamburg and from Frankfurt to Johannesburg.

Solid lines: FLUKA simulation

Radiation sources in space

Galactic Cosmic Rays

spectrum: 87% protons, 12% He ions and 1% heavier ions (in fluence) with peaks at 1 GeV/n

flux: 4 particles/(cm^2 s) at solar min.

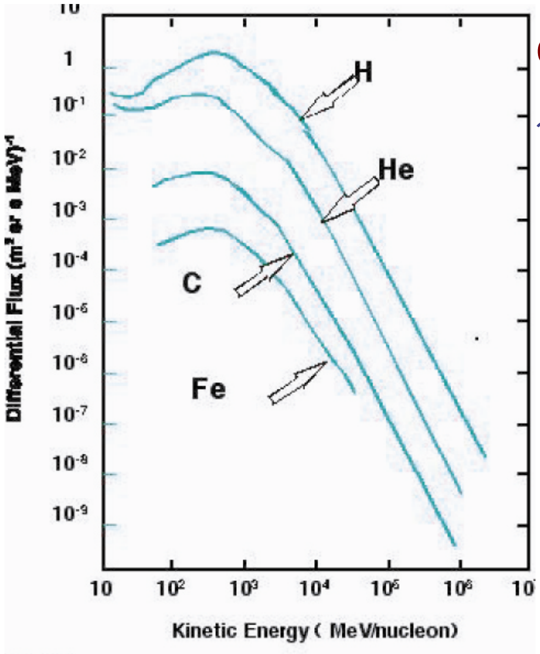

dose:

~1 mSv/day

NASA pub. 1998

Solar Particle Events

spectrum: 90% protons, 10% heavier ions with energy mainly below

flux: up to ~10^{10} particles/cm^2 in some hrs.

dose: order of Sv, strongly dependent on shielding and organ

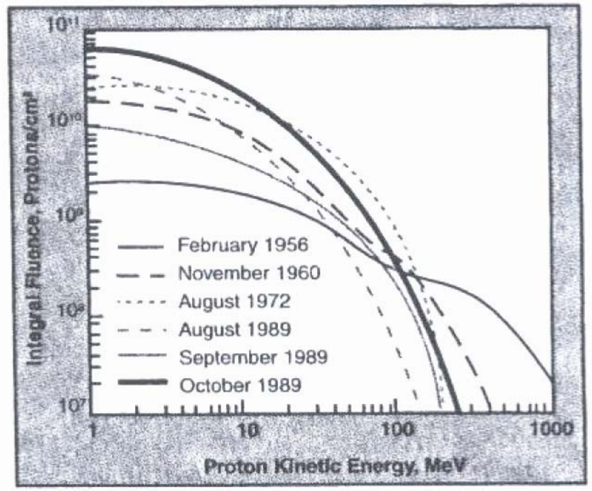

NASA pub. 1998

Dose rates in different missions

Shuttle  0.23 mSv/day

ISS  0.5-1 mSv/day

Apollo 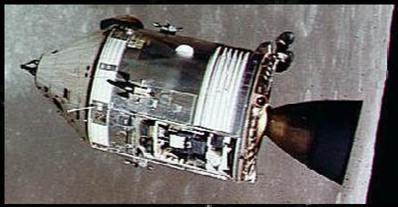 1.3 mSv/day

by comparison: an intercontinental flight rarely implies doses larger than 0.1 mSv; the radiation background on Earth is ≈ mSv/*year*

Methods

Quality factors

Yields of "Complex Lesions"

GCR and SPE spectra → **FLUKA** →

- Dose
- Dose Equivalent
- "Biological Dose"

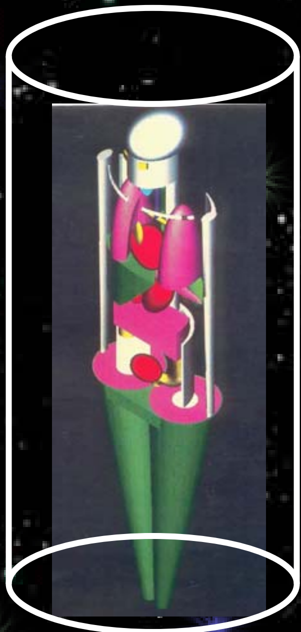

mathematical phantom

(Pellicciono et al.)

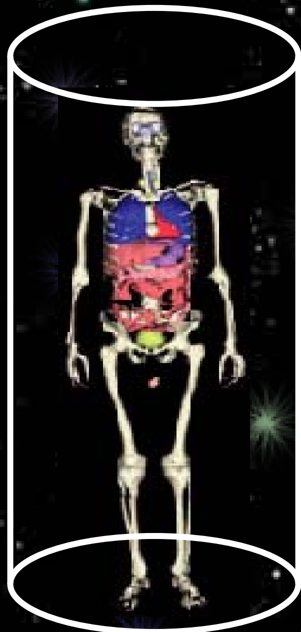

"voxel" phantom

(Zankl et al.)

Aug. 1972 SPE - calculated skin doses

dose (Gy)

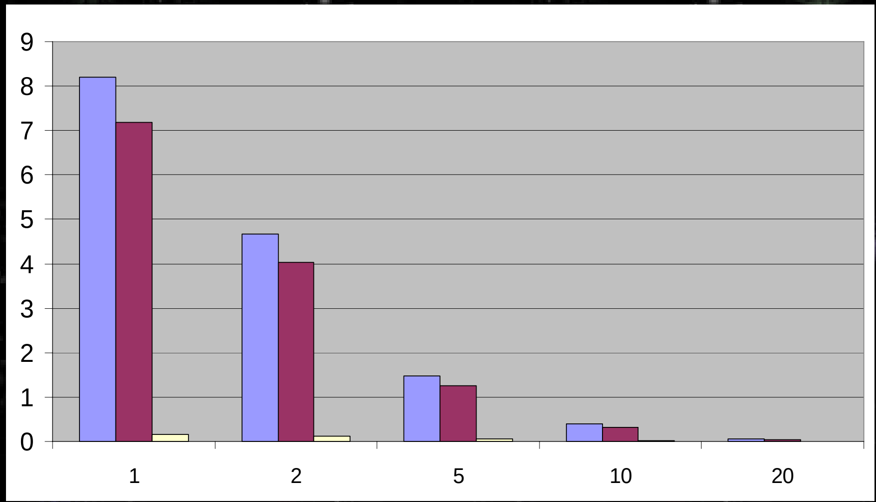

Al shield thickness (g/cm²)

dose equivalent (Sv)

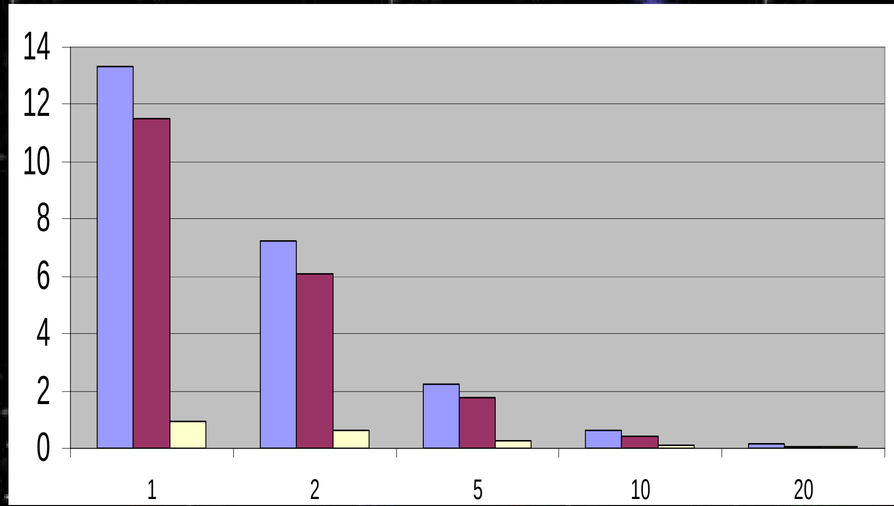

Al shield thickness (g/cm²)

"biological" dose (CLs/cell)

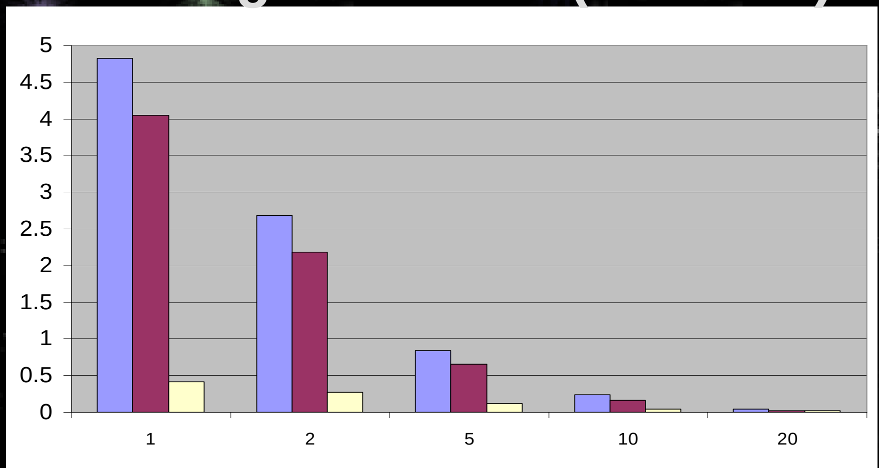

Al shield thickness (g/cm²)

- ***dramatic dose decrease with increasing shielding (i.e. from 13.3 to 0.62 Sv in the range 1-10 g/cm²)***
- ***major contribution from primary protons (the role of nuclear reaction products is not negligible only for equivalent and "biological" dose)***

Aug. 1972 SPE - skin vs. internal organs

dose equivalent to *skin* (Sv)

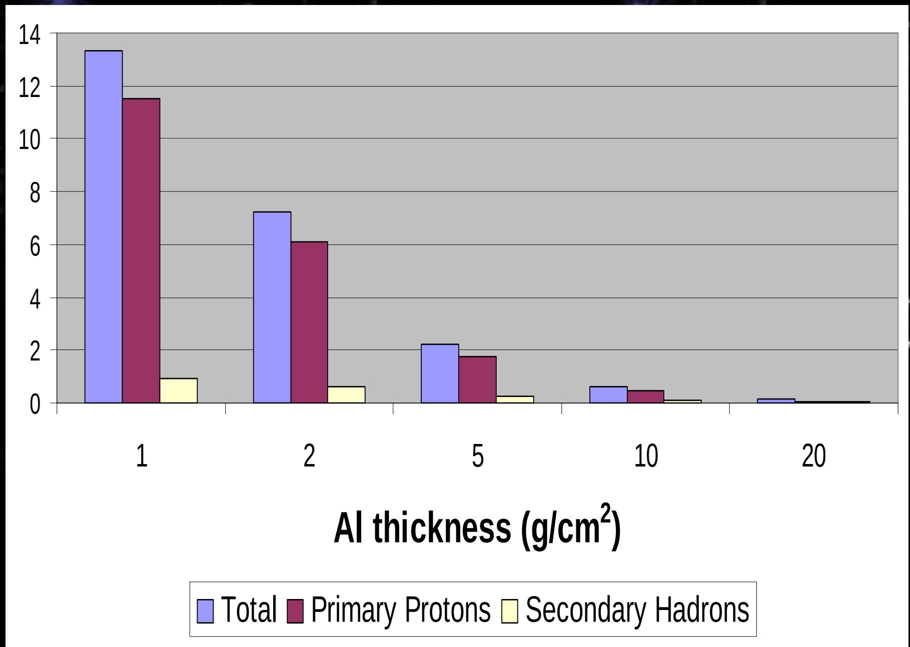

dose equivalent to *liver* (Sv)

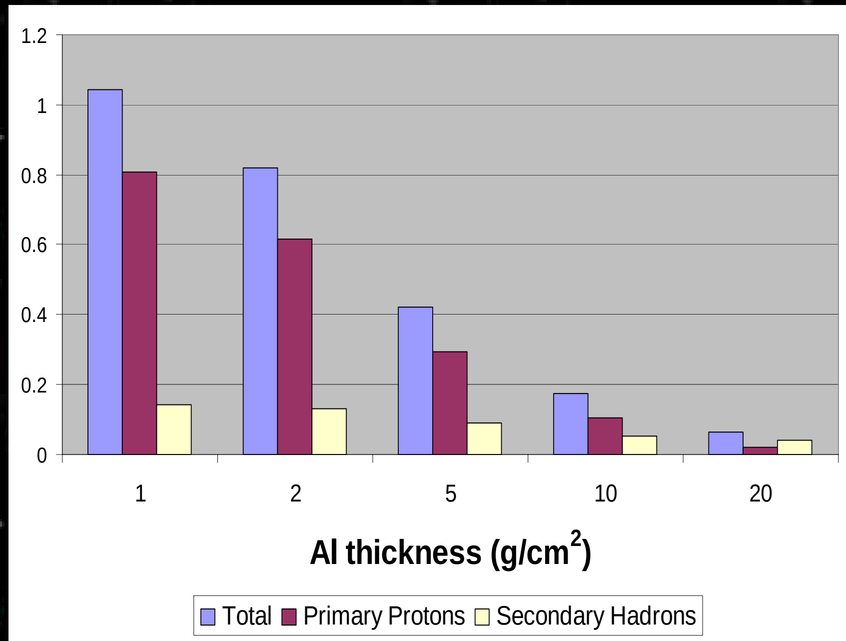

- ***much lower doses to liver than to skin (e.g. 1.0 vs. 13.3 Sv behind 1 g/cm^2 Al)***
- ***larger relative contribution of nuclear reaction products for liver than for skin (e.g. 14% vs. 7% behind 1 g/cm^2 Al)***

Galactic C.R.

RBM-averaged doses behind 1g/cm² Al shielding: role of the various spectrum components

al RBM-averaged dose equivalent = 1.2 mSv/d

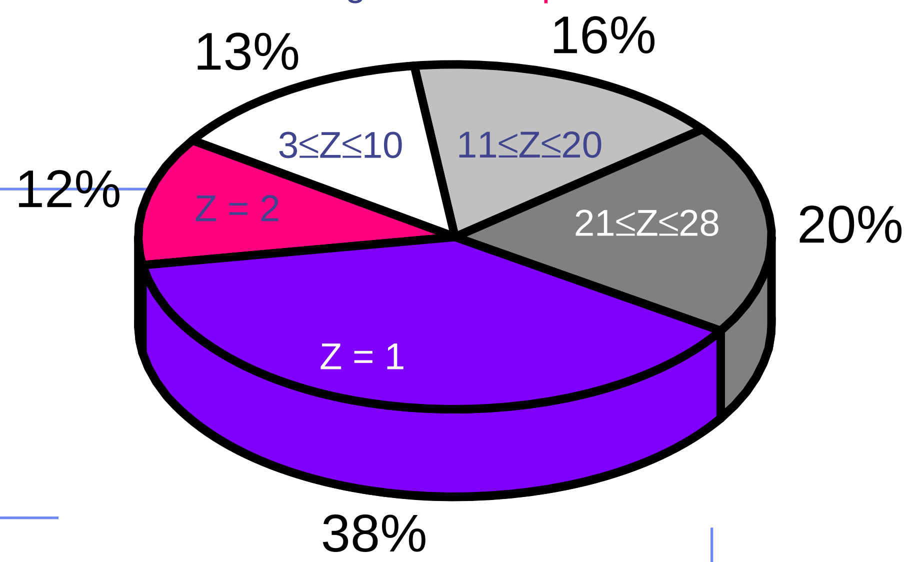

Total RBM-averaged absorbed dose = 0.5 mGy/d

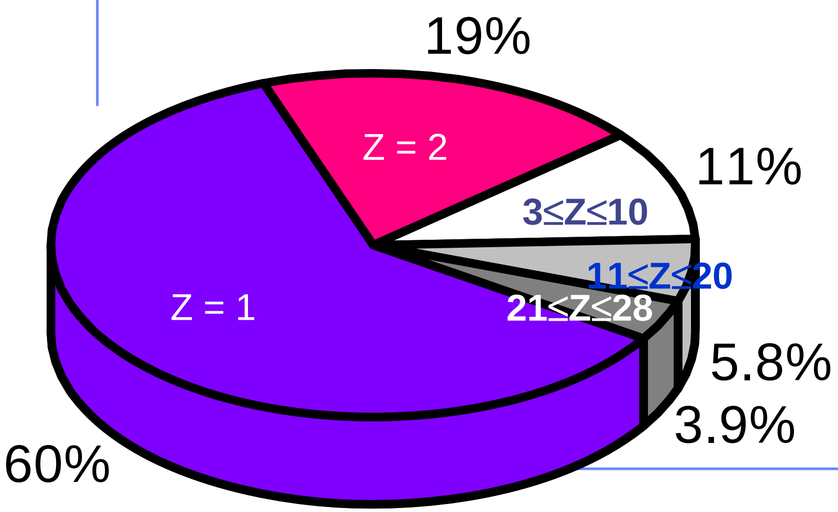

Total RBM-averaged “biological dose” = 0.4 * 10^{-3} CLs/d

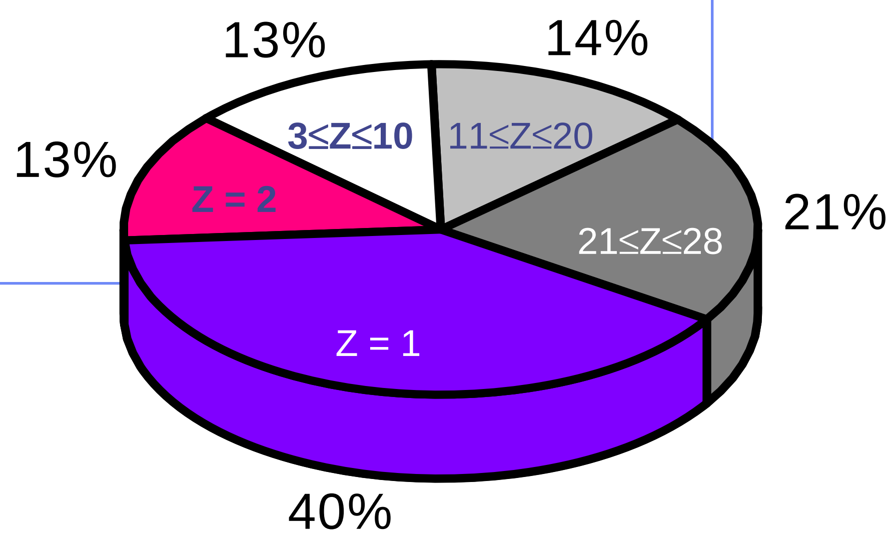

GCR solar min. - skin vs. internal organs

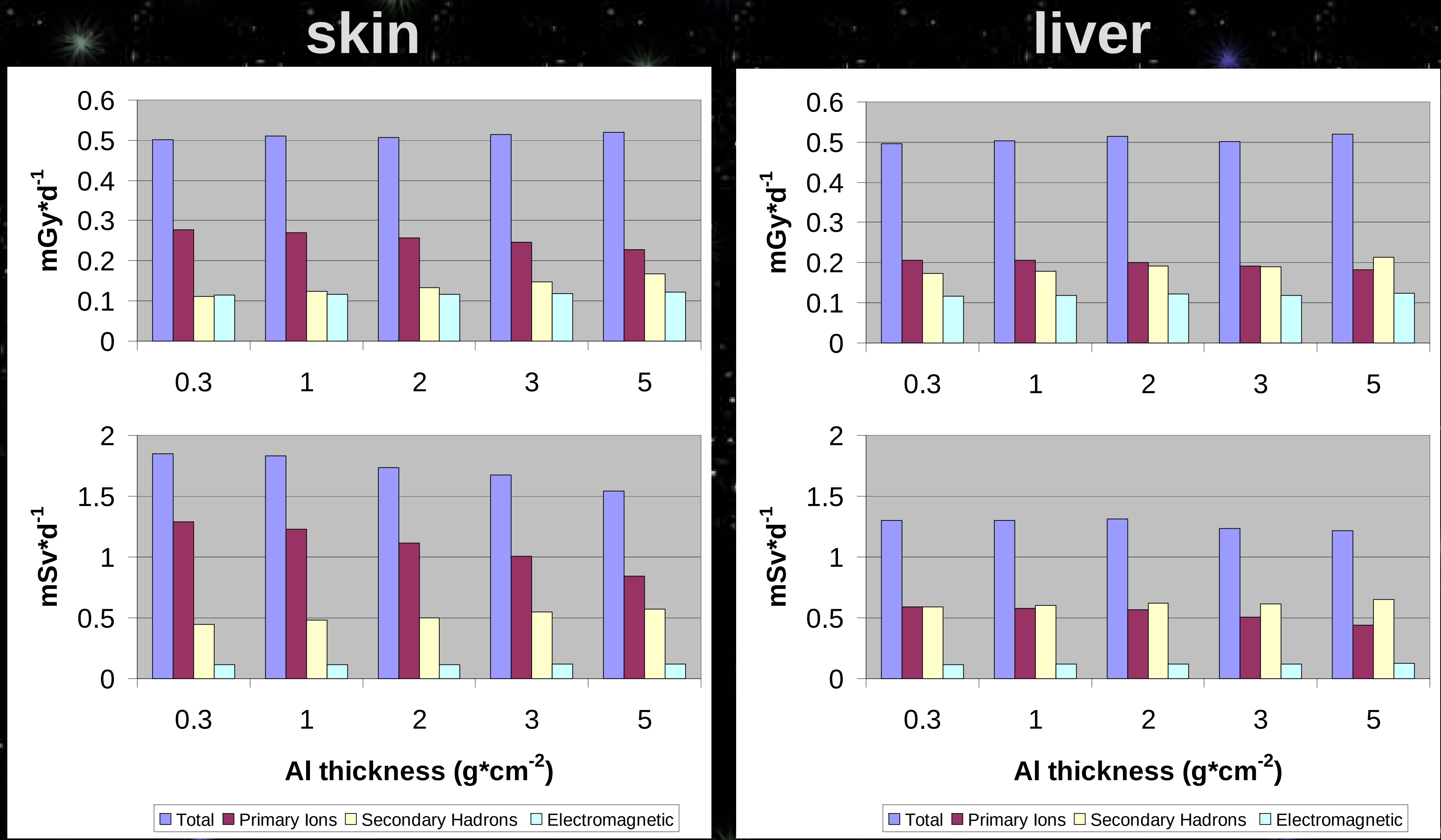

with respect to skin, internal organs have: 1) similar dose but smaller dose equivalent (~ 1.3 vs. 1.7 mSv/day); 2) larger relative contributions from nuclear interaction products

GCR at solar min. - annual effective dose

Al (g/cm^2)	male dose (Sv)	fem. dose (Sv)
0.3	0.47	0.43
1	0.47	0.44
2	0.46	0.41
3	0.43	0.41
5	0.42	0.42

the “effective dose” E is a sum over different organ doses, weighted by “tissue weighting factors”

gonads: 0.20

bone marrow, colon, lung, stomach: 0.12

bladder, breast, liver, esophagous, thyroid: 0.05

skin, bone surface: 0.01

others: 0.05

ICRP 60, 1990

Therapy related features

With the contribution of:

K.Parodi, H.Paganetti, T.Bortfeld, W.Enghardt, F.Fiedler, F.Sommerer

Massachusetts General Hospital, Boston

Heidelberg, Ion Therapy Center, Germany

Rossendorf, Germany

CERN, Geneva, Switzerland

Part of the material presented in the following is still unpublished. I am able to show it thanks to the courtesy of K.Parodi and MGH . It is not included in the official file of this presentation

HadroTherapy applications of MC:

- Powerful for cross checking treatment plannings, (particularly for dis-homogeneities)
- Possibility of describing complex geometries including voxel structures imported out of raw CT scans
- Essential (offline or online) for understanding heavy ion fragmentation
- Without alternatives for nuclear reaction related issues, like online PET monitoring

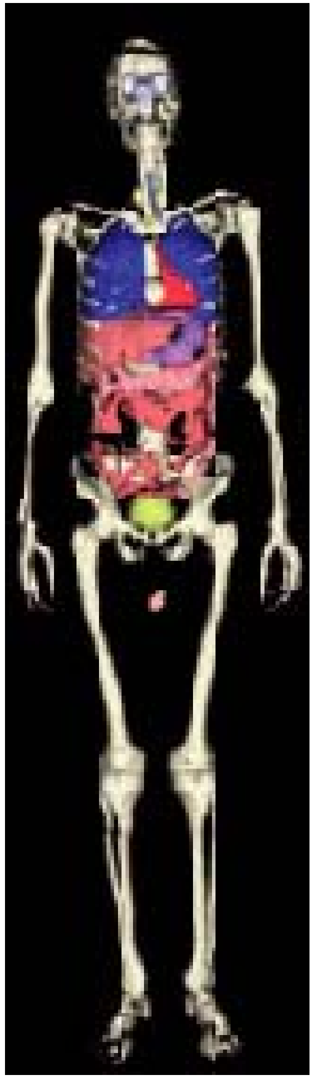

The GOLEM phantom
Petoussi-Henss et al, 2002

Bragg peaks vs exp. data: ^{20}Ne @ 670 MeV/n

Dose vs depth distribution for 670 MeV/n ^{20}Ne ions on a water phantom.
The green line is the FLUKA prediction
The symbols are exp data from LBL and GSI

Exp. Data
Jpn.J.Med.Phys. 18, 1,1998

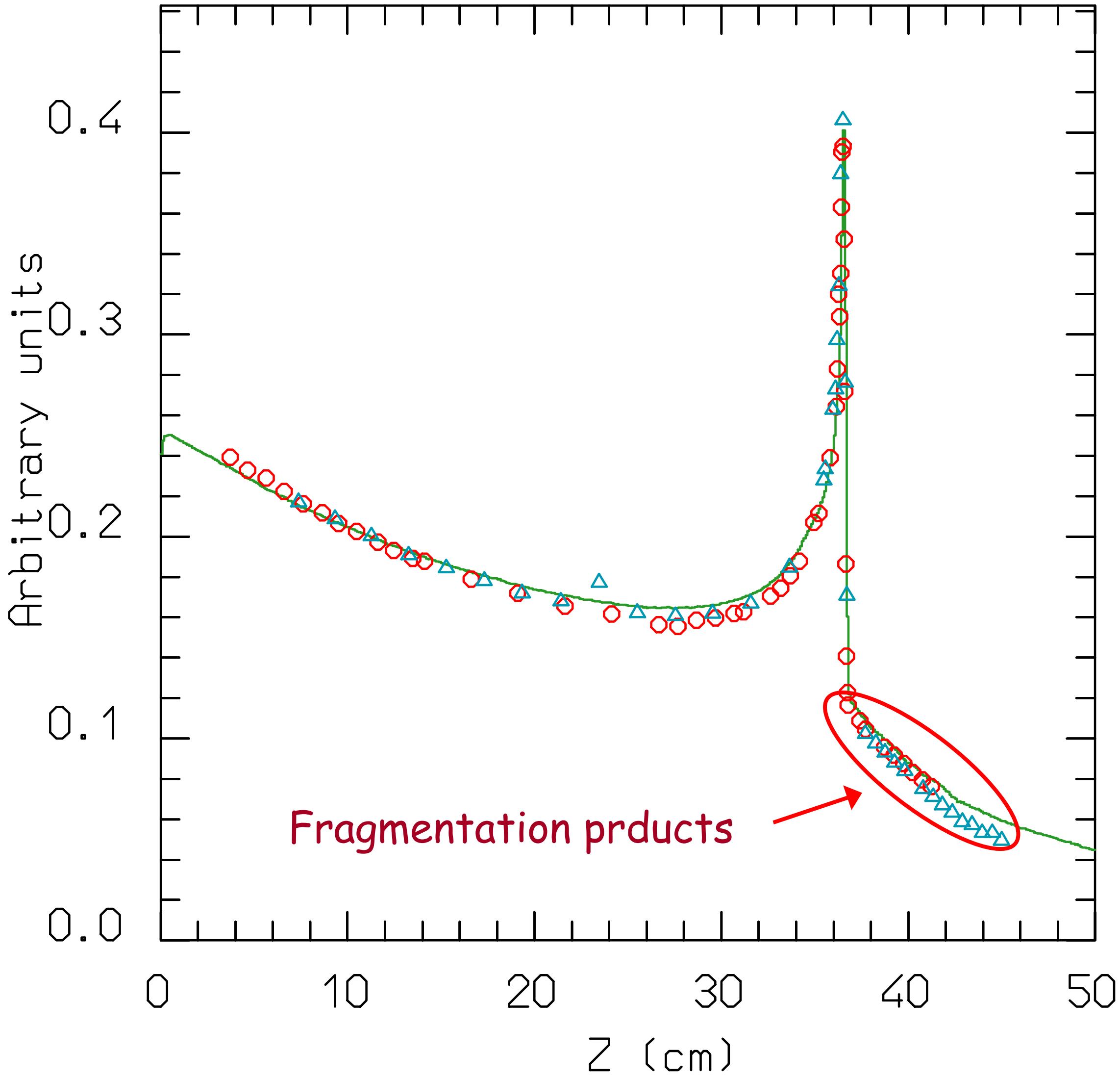

Bragg peaks vs exp. data: ^{12}C @ 270 & 330 MeV/n

Dose vs depth distribution for 270 and 330 MeV/n ^{12}C ions on a water phantom.
The full green and dashed blue lines are the FLUKA predictions
The symbols are exp data from GSI

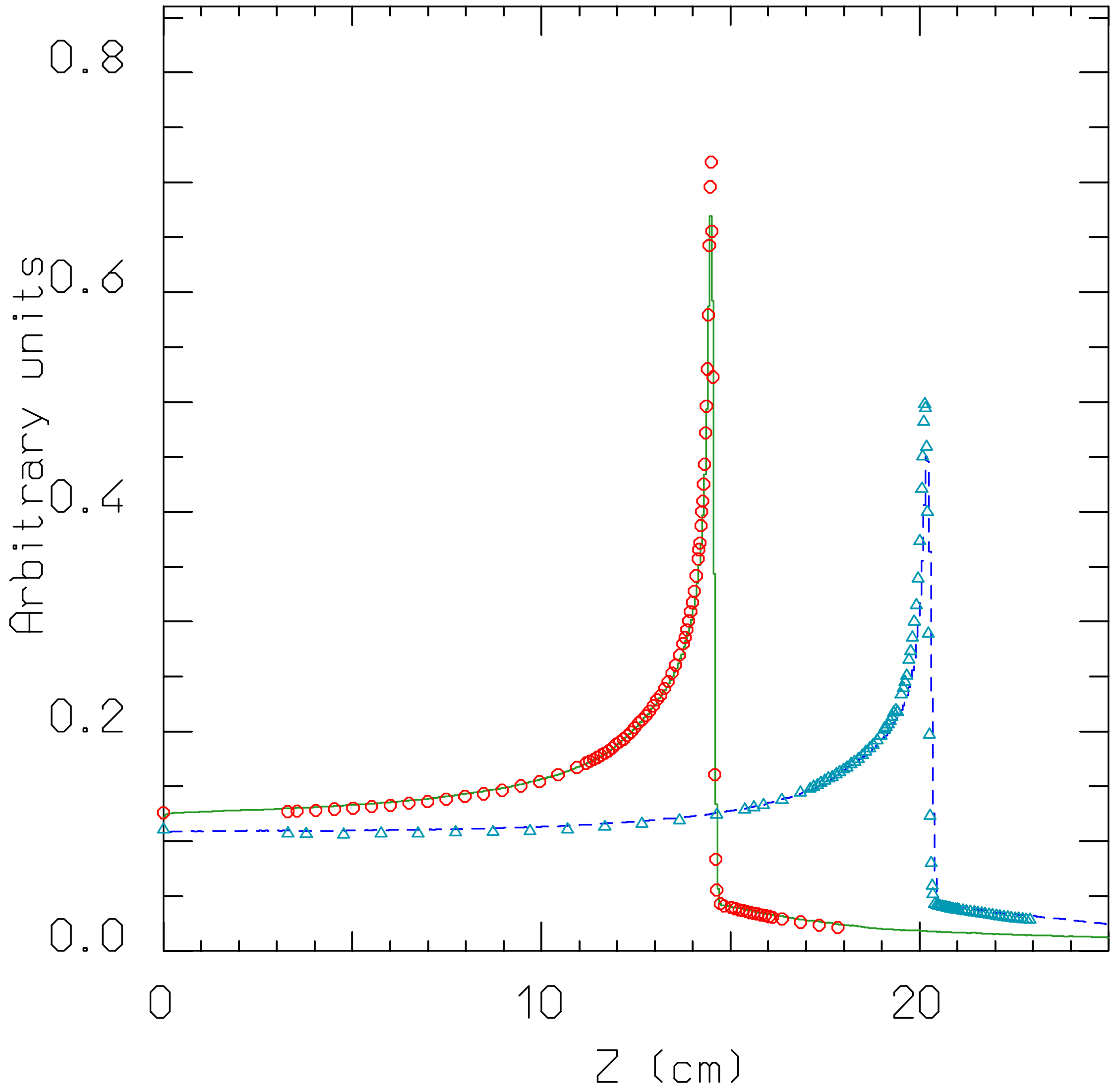

Exp. Data Jpn.J.Med.Phys. 18, 1,1998

Bragg peaks vs exp. data: ^{12}C @ 270 MeV/n

Close-up of the dose vs depth distribution for 270 MeV/n ^{12}C ions on a water phantom.

The green line is the FLUKA prediction with the nominal 0.15% energy spread

The dotted light blue line is the prediction for no spread, and the dashed blue one the prediction for *I* decreased by 1 eV

Exp. Data
Jpn.J.Med.Phys. 18, 1,1998

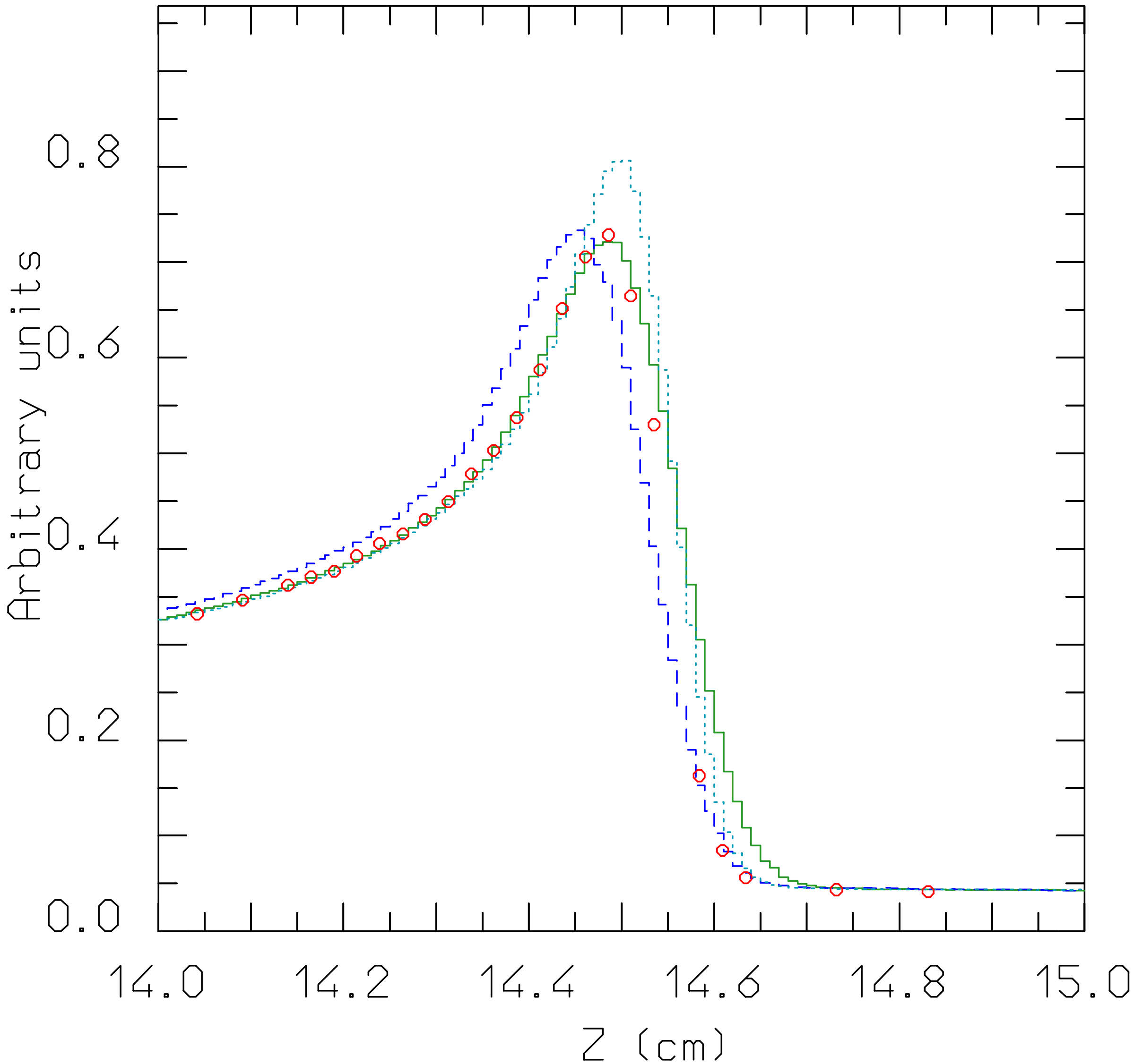

In-beam treatment control with PET:

Final goal: simulation of β+ emitters generated during the irradiation
→ In-beam treatment plan verification with PET

337 Mev/u ^{12}C on water, after irradiation

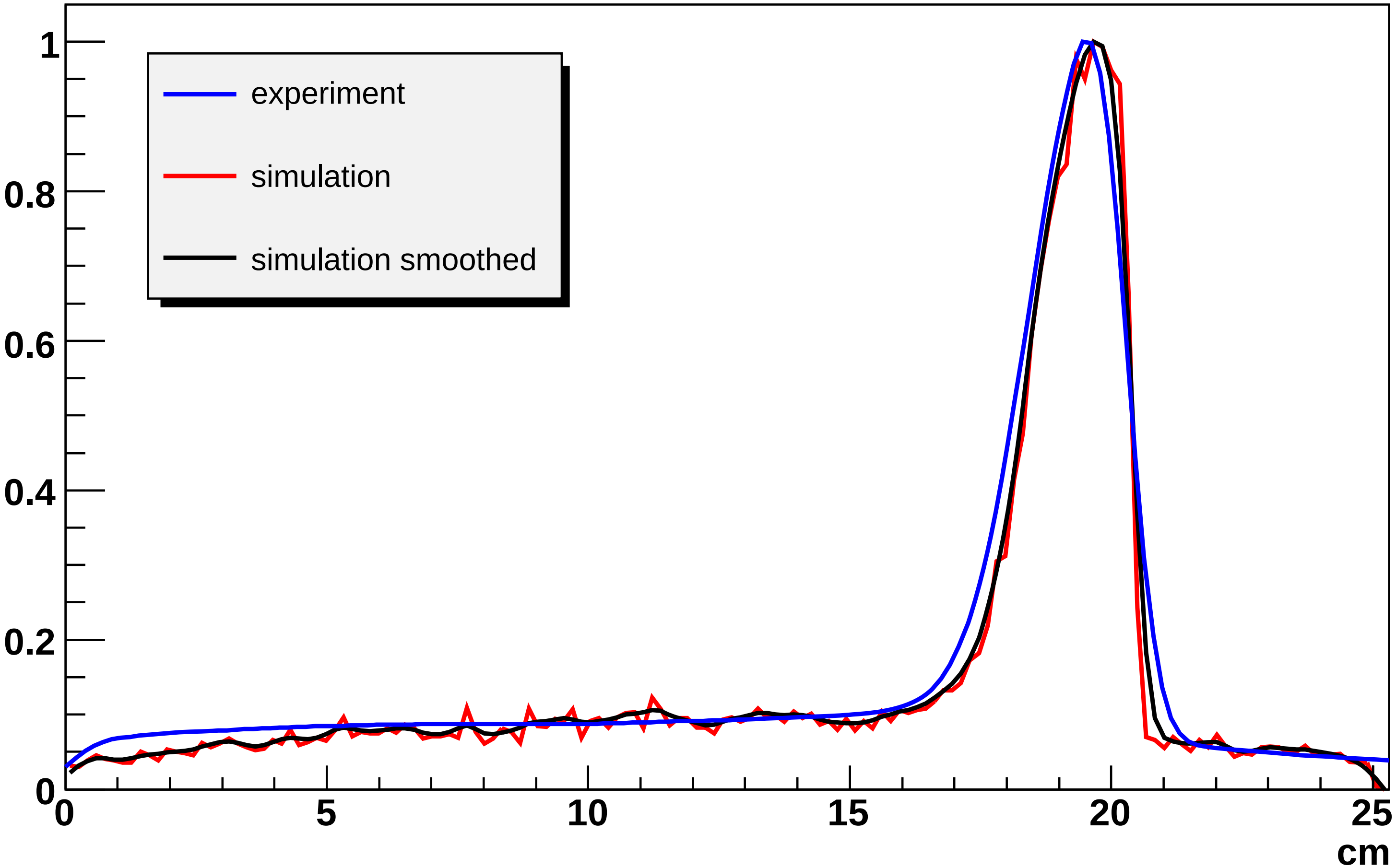

end